Human Molecular Genetics, 2004, Vol. 13, No. 14 ***1487–1503***
DOI: 10.1093/hmg/ddh160
Advance Access published on May 26, 2004

Expression profiling of the developing and mature $Nrl^{-/-}$ mouse retina: identification of retinal disease candidates and transcriptional regulatory targets of Nrl

Shigeo Yoshida[1,†,‡], Alan J. Mears[1,†,¶], James S. Friedman[1], Todd Carter[4], Shirley He[1], Edwin Oh[1], Yuezhou Jing[2], Rafal Farjo[1,§], Gilles Fleury[5], Carrolee Barlow[4,‖], Alfred O. Hero[2] and Anand Swaroop[1,3,*]

[1]Department of Ophthalmology and Visual Sciences, [2]Departments of EECS, Biomedical Engineering and Statistics and [3]Department of Human Genetics, University of Michigan, Ann Arbor, MI, USA, [4]The Salk Institute for Biological Studies, San Diego, California, USA and [5]Service des Mesures Ecole Supérieure d'Electricité, Gif-sur-Yvette, France

Received March 20, 2004; Revised and Accepted May 14, 2004

The rod photoreceptor-specific neural retina leucine zipper protein Nrl is essential for rod differentiation and plays a critical role in regulating gene expression. In the mouse retina, rods account for 97% of the photoreceptors; however, in the absence of Nrl ($Nrl^{-/-}$), no rods are present and a concomitant increase in cones is observed. A functional all-cone mouse retina represents a unique opportunity to investigate, at the molecular level, differences between the two photoreceptor subtypes. Using mouse GeneChips (Affymetrix), we have generated expression profiles of the wild-type and $Nrl^{-/-}$ retina at three time-points representing distinct stages of photoreceptor differentiation. Comparative data analysis revealed 161 differentially expressed genes; of which, 78 exhibited significantly lower and 83 higher expression in the $Nrl^{-/-}$ retina. Hierarchical clustering was utilized to predict the function of these genes in a temporal context. The differentially expressed genes primarily encode proteins associated with signal transduction, transcriptional regulation, intracellular transport and other processes, which likely correspond to differences between rods and cones and/or retinal remodeling in the absence of rods. A significant number of these genes may serve as candidates for diseases involving rod or cone dysfunction. Chromatin immunoprecipitation assay showed that in addition to the rod phototransduction genes, Nrl might modulate the promoters of many functionally diverse genes *in vivo.* Our studies provide molecular insights into differences between rod and cone function, yield interesting candidates for retinal diseases and assist in identifying transcriptional regulatory targets of Nrl.

INTRODUCTION

The mammalian retina contains a diverse array of anatomically and functionally distinct neurons (1). Rod and cone photoreceptors account for >70% of all cells in the retina. In most mammals, rods are almost 20-fold more in number compared with cones though their distribution may vary greatly in different regions (2). Photoreceptors are highly metabolically active post-mitotic neurons; it is estimated that almost 10 billion opsin molecules are synthesized per

*To whom correspondence should be addressed at: Department of Ophthalmology and Visual Sciences and Department of Human Genetics, W.K. Kellogg Eye Center, University of Michigan, 1000 Wall Street, Ann Arbor, MI 48105-0714, USA. Tel: +1 7347633731; Fax: +1 7346470228; Email: swaroop@umich.edu
†The authors wish it to be known that, in their opinion, the first two authors should be regarded as joint First Authors.
‡Present address: Department of Ophthalmology, Kyushu University Graduate School of Medical Sciences, Fukuoka, Japan.
¶Present address: University of Ottawa Eye Institute and Ottawa Health Research Institute, Ottawa, Ontario, Canada.
§Present address: Department of Cell Biology, University of Oklahoma Health Sciences Center, Oklahoma City, OK, USA.
‖Present address: Merck Research Laboratories, San Diego, CA, USA.

second in each human retina (3). Hence, it is not surprising that altered expression or function of opsin and other phototransduction proteins results in photoreceptor degeneration (4–6). The transcriptional regulatory networks underlying photoreceptor differentiation and function are understood poorly.

The neural retina leucine zipper (Nrl) protein, a transcription factor of the Maf-subfamily, is expressed specifically in the rod photoreceptors of the retina (7,8) and the pineal gland (A.J. Mears and A. Swaroop, unpublished data). Nrl has been shown to interact with the retina-specific homeodomain protein Crx (9) and regulate the expression of rhodopsin (10) and rod cGMP-phosphodiesterase α- (11) and β-subunits (12). In humans, missense mutations of *NRL* are associated with autosomal dominant retinitis pigmentosa (13–17), and in at least one instance (Ser50Thr mutation), the disease may be a result of increased activity of the NRL protein. Targeted deletion of Nrl in mice results in a complete loss of rods and a supernormal S-cone function, as demonstrated by histology, immunocytochemistry, ERG and expression analysis (18). These observations led to the hypothesis that Nrl plays a critical role in the differentiation of rod photoreceptors, and in its absence, the immature photoreceptors adopt an S-cone phenotype (18). The retina of the $Nrl^{-/-}$ mouse exhibits similarities to the *Nr2e3*^{rd7} mouse (19,20) and its corresponding human disease enhanced S-cone syndrome (21). One plausible explanation of the phenotypic overlap is that Nrl directly or indirectly regulates Nr2e3 expression, which is undetectable in the $Nrl^{-/-}$ mouse retina (18).

Although several transcription factors have been implicated in photoreceptor differentiation or gene regulation (22–25), their direct impact on the photoreceptor transcriptome has not been elucidated. Microarray-based global expression profiling of tissues from mice deficient in a transcription factor gene can point to downstream regulatory targets and provide candidate genes for functional studies and cloning of disease loci (26). This approach has been utilized successfully in studies of the mouse retina (27,28). The $Nrl^{-/-}$ retina is particularly amenable to this analysis because of its dramatic phenotype of no rods and enhanced cones. In the retina of $Nrl^{-/-}$ mice, rod bipolar cells have normal morphology, pattern of staining and lamination, and form functional connections with the cones, and the axonal arbors of horizontal cells and AII amacrine cells maintain a normal morphology and stratification pattern (E. Strettoi, A.J. Mears and A. Swaroop, unpublished data). We, therefore, hypothesize that the comparative analysis of gene profiles from the wild-type and $Nrl^{-/-}$ retina will, to a large extent, reveal expression differences between rod and cone transcriptomes. Based on our initial analysis of phototransduction genes (18), we predict that transcripts encoding rod photoreceptor proteins would be expressed at lower levels (or undetectable) in the $Nrl^{-/-}$ retina. Conversely, the transcripts specific to the normally sparse population of cones are expected to be enriched in the $Nrl^{-/-}$ retina.

Here, we report the gene expression profiles, obtained by using Affymetrix GeneChips (MGU74Av2), of the wild-type and $Nrl^{-/-}$ retina at three time-points (post-natal days 2 and 10, and 2 months). After data normalization by robust multichip average algorithm (RMA) (29) and ranking the statistically validated genes with a minimum 1.5 average fold-change (AFC) in expression, we have identified 161 differentially expressed genes, which include the known rod- or cone-specific genes represented on these chips. Functional annotation suggests a wide spectrum of physiological changes that likely correspond to differences between rods and cones and/or remodeling of retina in the absence of rods. Our analysis suggests that ~25% of all differentially expressed genes identified in this study are either associated with (15) or are candidates (26) for retinal diseases. Using chromatin immunoprecipitation (ChIP) analysis, a significant proportion of the top ranked genes showing reduced expression in the $Nrl^{-/-}$ retina are demonstrated to be putative direct targets of Nrl, indicating the breadth of its influence on the rod transcriptome.

RESULTS

Identification of differentially expressed genes in the $Nrl^{-/-}$ retina

The three time-points, P2, P10 and 2 months, were chosen to cover distinct critical stages of photoreceptor development in mouse. In the wild-type retina, at P2 many retinal progenitor cells are still exiting the cell cycle and a majority of these will become rods (30). The photopigment of the rod photoreceptors, rhodopsin, is first detected at P4. At P10, retinogenesis is complete, the cells are undergoing terminal differentiation and photoreceptor outer segments are beginning to form. We chose 2 months of age as another suitable time-point as the retina is structurally and functionally matured and yet old enough to avoid any potential delayed differentiation effects which may occur due to the re-specification of the photoreceptor cell types in the $Nrl^{-/-}$ retina.

To facilitate statistical analysis and identification of 'true' positives, four replicate MGU74Av2 GeneChips were utilized for each time-point and strain. Based on absent/present calls (MAS5 analysis), ~60% of the probesets (out of ~12 400) were reported as present or marginally detectable in at least one of the 12 wild-type GeneChips, consistent with other studies analyzing single tissue types. Signal quantification and normalization were performed using RMA, a reliable and effective algorithm in control studies (31,32). The normalized data were then analyzed with a robust two-step procedure to identify statistically significant differentially expressed genes. Due to the tendency of microarrays to quantitatively underestimate fold-change in expression and since RMA normalization compresses the signals (and resulting ratios), an empirical 1.5 AFC cut-off was selected as the minimum fold-change (minfc) for statistical analysis. Using these criteria and after removal of those scored as absent on all 24 chips, a total of 173 probesets were reported as differentially expressed for at least one of the three time-points (i.e. *P*-value <1). Of these, 86 show decreased (Table 1, down-regulated genes) and 87 increased (Table 1, up-regulated genes) expression in the $Nrl^{-/-}$ retina. The differentially expressed genes are ranked based on increasing false discovery rate confidence interval (FDRCI) *P*-values, which are similar to FDR *P*-values except that they account for a specified minfc level in

Table 1. Summary of microarray-based expression

Probeset	Accession no.	Gene description	Name	P2 AFC	P10 AFC	2M AFC	*P*-value
Down-regulated genes							
96134_at	NM_139292	Deleted in polyposis 1-like 1	Dp1l1	—	−10.12	−15.94	0.0001
96567_at	NM_145383	Rhodopsin	Rho	—	−24.82	−41.30	0.0001
94701_at	NM_008806	Phosphodiesterase 6B, cGMP, rod receptor, beta polypeptide	Pde6b	*−2.29*	−37.30	−25.00	0.0002
95389_at	XM_132106	Cyclic nucleotide gated channel alpha 1	Cnga1	—	−7.25	−13.63	0.0004
93453_at	NM_009073	Retinal outer segment membrane protein 1	Rom1	−2.17	−5.32	−3.27	0.0004
94853_at	NM_008142	Guanine nucleotide binding protein, beta 1	Gnb1	*1.17*	−4.01	−8.12	0.0004
98531_g_at	NM_013525	Growth arrest specific 5	Gas5	*−1.15*	*−2.08*	−6.28	0.0008
94139_at	NM_024458	Phosducin	Pdc	−4.41	−3.84	−1.91	0.0008
93330_at	NM_007472	Aquaporin 1	Aqp1	—	*−1.33*	−7.84	0.0011
104592_i_at	NM_025282	Myocyte enhancer factor 2C	Mef2c	—	—	−4.18	0.0029
161871_f_at	NM_145383	Rhodopsin	Rho**	—	−2.95	−7.80	0.0030
94150_at	NM_009118	Retinal S-antigen	Sag	−5.07	−4.10	*−1.20*	0.0037
99860_at	NM_008140	Guanine nucleotide binding protein, alpha transducing 1	Gnat1	*−1.19*	−55.61	−216.35	0.0046
95755_at	NM_011733	Cold shock domain protein A	Csda	*1.13*	*−1.51*	−2.25	0.0059
161525_f_at	NM_009073	Retinal outer segment membrane protein 1	Rom1**	*1.04*	−4.76	−3.70	0.0060
162167_f_at	NM_008806	Phosphodiesterase 6B, cGMP, rod receptor, beta polypeptide	Pde6b**	—	−3.74	−4.99	0.0060
93533_at	NM_026899	RIKEN cDNA *1500011L16* gene	1500011L16Rik	*−1.06*	−2.62	*−1.72*	0.0065
93699_at	NM_015810	Polymerase (DNA directed), gamma 2, accessory subunit	Polg2	*−1.01*	−1.73	−3.64	0.0069
93094_at	NM_007672	Cerebellar degeneration-related 2	Cdr2	*−1.07*	−2.99	−5.47	0.0080
104591_g_at	NM_025282	Myocyte enhancer factor 2C	Mef2c**	—	—	−2.53	0.0080
101923_at	NM_013737	Phospholipase A2, group VII	Pla2g7	*−1.03*	−2.57	*−1.82*	0.0115
96831_at	NM_028295	Protein disulfide isomerase-related	Pdir-pending	*−1.02*	*−1.14*	−2.68	0.0120
103895_at	NM_145930	Expressed sequence AW549877	AW549877	*1.03*	−2.08	*−1.30*	0.0130
92796_at	NM_007431	Alkaline phosphatase 2, liver	Akp2	—	−3.10	−3.17	0.0144
100696_at	NM_008805	Phosphodiesterase 6A, cGMP-specific, rod, alpha	Pde6a	—	*−2.12*	−2.95	0.0160
102890_at	NM_009228	Syntrophin, acidic 1	Snta1	*−1.07*	−2.74	−2.37	0.0194
160273_at	NM_007565	Zinc finger protein 36, C3H type-like 2	Zfp36l2	*1.41*	−1.96	−3.68	0.0197
160134_at	XM_129394	Adiponectin receptor 1	AdipoR1	*−1.20*	*−1.42*	−2.73	0.0248
98853_at	NM_008867	Phospholipase A2, group IB, pancreas, receptor	Pla2g1br	—	−3.13	−2.82	0.0254
100946_at	XM_286803	Heat shock protein 1B	Hspa1b	—	*−1.19*	−3.17	0.0269
104590_at	NM_025282	Myocyte enhancer factor 2C	Mef2c**	—	—	−3.66	0.0295
93875_at	XM_207062	Heat shock protein 1A	Hspa1a	*−1.05*	*−1.19*	−2.62	0.0296
92691_at	NM_028392	RIKEN cDNA *2900026H06* gene	2900026H06Rik	*−1.41*	−3.19	*−1.23*	0.0340
97730_at	NM_007378	ATP-binding cassette, sub-family A (ABC1), member 4	Abca4	*−1.43*	−2.76	−2.22	0.0347
103733_at	AK013486	RIKEN cDNA *2900006A08* gene	2900006A08Rik	*1.00*	*−1.49*	−1.96	0.0383
102044_at	NM_018865	WNT1 inducible signaling pathway protein 1	Wisp1	—	*−1.23*	−3.33	0.0479
102612_at	NM_008736	Neural retina leucine zipper gene	Nrl	—	−2.59	−2.48	0.0510
99392_at	NM_009397	Tumor necrosis factor, alpha-induced protein 3	Tnfaip3	—	−2.12	−4.52	0.0580
95541_at	NM_138587	DNA segment, Chr 6, Wayne State University 176, expressed	D6Wsu176e	*1.00*	*−1.43*	−3.27	0.0650
160807_at	NM_053014	1-Acylglycerol-3-phosphate *O*-acyltransferase 3	Agpat3	*−1.08*	*−1.10*	−2.27	0.0700
98300_at	NM_009785	Calcium channel, voltage dependent, alpha2/delta subunit 3	Cacna2d3	—	*1.00*	−2.08	0.0780
93390_g_at	NM_008935	Prominin 1	Prom1	*1.00*	−1.86	*−1.64*	0.0810
160597_at	NM_133825	DNA segment, Chr 1, ERATO Doi 622, expressed	D1Ertd622e	*1.09*	*−1.33*	−2.46	0.0934
160693_at	NM_054097	Phosphatidylinositol-4-phosphate 5-kinase, type II, gamma	Pip5k2c	*−1.08*	−1.90	−2.21	0.0980
97890_at	NM_011361	Serum/glucocorticoid regulated kinase	Sgk	*−1.09*	*−1.02*	−2.69	0.0980
93328_at	NM_008230	Histidine decarboxylase	Hdc	—	—	−2.12	0.1070
93887_at	NM_010820	Multiple PDZ domain protein	Mpdz	*1.06*	*−1.50*	−2.60	0.1084
104206_at	NM_026153	RIKEN cDNA *0610012A05* gene	0610012A05Rik	*−2.07*	−5.70	−2.66	0.1195
96596_at	NM_008681	N-myc downstream regulated-like	Ndrl	*−1.05*	−1.78	−2.64	0.1370
102292_at	NM_007836	Growth arrest and DNA-damage-inducible 45 alpha	Gadd45a	*1.10*	−2.15	−2.32	0.1450
160948_at	NM_008915	Protein phosphatase 3, catalytic subunit, gamma isoform	Ppp3cc	*1.01*	*−1.07*	−2.27	0.1578

Continued

Table 1. *Continued*

Probeset	Accession no.	Gene description	Name	P2 AFC	P10 AFC	2M AFC	*P*-value
97770_s_at	NM_138587	DNA segment, Chr 6, Wayne State University 176, expressed	D6Wsu176e**	*1.20*	*−1.27*	−2.84	0.1610
160464_s_at	NM_010884	N-myc downstream regulated 1	Ndr1	*−1.08*	−1.82	−2.60	0.1819
94739_at	NM_011643	Transient receptor potential cation channel, subfamily C, member 1	Trpc1	*1.00*	*−1.13*	−2.55	0.1948
97755_at	NM_007878	Dopamine receptor 4	Drd4	—	−4.54	−2.46	0.2070
101151_at	NM_009038	Recoverin	Rcvrn	—	−2.37	−2.12	0.2120
97357_at	AK044589	Myocyte enhancer factor 2C	Mef2c**	—	—	−2.39	0.2140
96354_at	NM_020007	Muscleblind-like (*Drosophila*)	Mbnl1	*1.05*	−2.02	*−1.47*	0.2530
95603_at	NM_138595	Glycine decarboxylase	Gldc	*−1.13*	−2.15	*1.17*	0.2840
102413_at	NM_057173	LIM domain only 1	Lmo1	*−1.16*	*−1.54*	−1.87	0.2940
98993_at	NM_012023	Protein phosphatase 2, regulatory subunit B (B56), gamma isoform	Ppp2r5c	*−1.08*	*−1.45*	−2.12	0.3280
93130_at	NM_183212	Hypothetical protein D030064A17	D030064A17	*1.04*	*−1.68*	−1.96	0.3570
93389_at	NM_008935	Prominin 1	Prom1**	*1.01*	−1.82	*−1.64*	0.3640
93202_at	NM_011851	5′ Nucleotidase, ecto	Nt5e	*1.09*	*−2.07*	−2.65	0.3720
95285_at	XM_128499	KRAB box containing zinc finger protein	KRIM-1	*1.05*	*−1.12*	−1.84	0.4030
102352_at	NM_134189	*N*-Acetylgalactosaminyltransferase 9	Galnt9	*1.03*	*−1.28*	−1.80	0.4760
98569_at	NM_146118	Mitochondrial Ca^{2+}-dependent solute carrier	Mcsc-pending	*−1.18*	*−1.47*	−1.98	0.4830
99461_at	NM_008225	Hematopoietic cell specific Lyn substrate 1	Hcls1	—	—	−1.90	0.4850
97579_f_at	NM_027010	Crystallin, gamma F	Crygf	*1.82*	*2.46*	−3.51	0.4940
160808_at	NM_031869	Protein kinase, AMP-activated, beta 1 non-catalytic subunit	Prkab1	*−1.15*	*−1.55*	−2.13	0.5120
101308_at	NM_008420	Potassium voltage gated channel, Shab-related subfamily, member 1	Kcnb1	—	−2.14	−2.43	0.5120
103026_f_at	NM_007777	Crystallin, gamma E	Cryge	*1.74*	*2.24*	−3.07	0.5220
98524_f_at	AK008780	RIKEN cDNA *2210039B01* gene	2210039B01Rik	*1.02*	*−1.58*	−2.26	0.5290
98329_at	XM_193953	6-Phosphofructo-2-kinase/ fructose-2,6-biphosphatase 2	Pfkfb2	—	*−1.47*	−1.77	0.5697
103460_at	NM_029083	HIF-1 responsive RTP801	Rtp801-pending	*1.00*	*−1.17*	−2.14	0.5980
100757_at	XM_194003	Calcium channel, voltage-dependent, beta 2 subunit	Cacnb2	—	−2.23	*−1.81*	0.6290
102835_at	NM_007459	Adaptor protein complex AP-2, alpha 2 subunit	Ap2a2	*1.02*	*−1.52*	−1.83	0.6490
99586_at	NM_009976	Cystatin C	Cst3	*−1.07*	−1.71	*−1.60*	0.6940
96156_at	AK003573	RIKEN cDNA *1110008H02* gene	1110008H02Rik	*−3.21*	−2.38	−4.42	0.7627
104171_f_at	NM_007776	Crystallin, gamma D	Crygd	*1.83*	*2.37*	−3.16	0.7652
96766_s_at	NM_019392	TYRO3 protein tyrosine kinase 3	Tyro3	*−1.16*	*−1.07*	−1.63	0.7750
101489_at	NM_009665	*S*-Adenosylmethionine decarboxylase 1	Amd1	*1.20*	*−1.04*	−1.80	0.8460
103922_f_at	NM_028057	Cytochrome b5 reductase 1 (B5R.1)	Cyb5r1-pending	*1.11*	*−1.42*	−2.04	0.8540
92790_at	NM_010655	Karyopherin (importin) alpha 2	Kpna2	*1.30*	*−1.35*	−1.97	0.8670
92607_at	NM_008590	Mesoderm specific transcript	Mest	*1.41*	*1.08*	−2.02	0.9058
101702_at	NM_011302	Retinoschisis 1 homolog (human)	Rs1h	—	−2.70	*−1.59*	0.9617
Up-regulated genes							
92237_at	NM_009107	Retinoid X receptor gamma	Rxrg	*−1.01*	2.50	2.92	0.0000
160893_at	NM_023121	Guanine nucleotide binding protein, gamma transducing activity pp 2	Gngt2	*1.14*	6.20	7.90	0.0001
98807_at	NM_008141	Guanine nucleotide binding protein, alpha transducing 2	Gnat2	*1.48*	7.20	7.58	0.0002
162287_r_at	NM_017474	Chloride channel calcium activated 3	Clca3	—	3.20	14.88	0.0003
99395_at	NM_007538	Opsin 1 (cone pigments), short-wave-sensitive	Opn1sw	*1.29*	8.43	9.40	0.0004
102151_at	NM_007419	Adrenergic receptor, beta 1	Adrb1	*1.16*	4.33	4.55	0.0007
98498_at	NM_007611	Caspase 7	Casp7	*1.06*	1.75	6.36	0.0017
98499_s_at	NM_007611	Caspase 7	Casp7**	*−1.05*	*1.67*	5.93	0.0023
96920_at	NM_019564	Protease, serine, 11 (Igf binding)	Prss11	*1.13*	2.30	*1.36*	0.0023
98427_s_at	NM_008689	Nuclear factor of kappa light chain gene enhancer in B-cells 1, p105	Nfkb1	*1.05*	1.81	3.05	0.0037
103198_at	AI848576	Expressed sequence AI848576	AI848576	—	2.37	*1.52*	0.0040
104346_at	NM_028250	Acyl-coenzyme A binding domain containing 6	Abdc6	*1.06*	*1.70*	2.67	0.0040
98918_at	NM_145367	Thioredoxin domain containing 5	Txndc5	*−1.09*	*1.17*	2.69	0.0047
160754_at	NM_011224	Muscle glycogen phosphorylase	Pygm	—	*1.25*	4.28	0.0050
98957_at	NM_023277	Junction adhesion molecule 3	Jam3	*1.03*	2.03	3.31	0.0052
98967_at	NM_021272	Fatty acid binding protein 7, brain	Fabp7	*1.12*	3.27	7.28	0.0065
95356_at	NM_009696	Apolipoprotein E	Apoe	*−1.16*	2.23	*1.70*	0.0066
101855_at	NM_010837	Microtubule-associated protein 6	Mtap6	*−1.09*	*1.52*	2.98	0.0070

Continued

Table 1. *Continued*

Probeset	Accession no.	Gene description	Name	P2 AFC	P10 AFC	2M AFC	*P*-value
104643_at	XM_109956	KIBRA protein	Kibra	*1.13*	5.51	5.98	0.0070
93482_at	AK020638	RIKEN cDNA *9530072E15* gene	9530072E15Rik	*1.08*	2.17	2.78	0.0080
102682_at	NM_007939	Eph receptor A8	Epha8	*−1.04*	2.65	*1.22*	0.0080
160828_at	XM_148966	Inhibin beta-B	Inhbb	*1.26*	2.83	—	0.0080
103038_at	NM_008189	Guanylate cyclase activator 1a (retina)	Guca1a	*−1.21*	5.65	*1.45*	0.0115
99238_at	NM_013530	Guanine nucleotide binding protein, beta 3	Gnb3	*1.46*	2.75	5.34	0.0130
98852_at	NM_178280	Sal-like 3 (*Drosophila*)	Sall3	*1.23*	3.46	2.63	0.0130
93290_at	NM_013632	Purine-nucleoside phosphorylase	Pnp	*1.47*	2.97	4.22	0.0139
100453_at	NM_007595	Calcium/calmodulin-dependent protein kinase II, beta	Camk2b	*1.01*	2.30	3.11	0.0166
94338_g_at	NM_008087	Growth arrest specific 2	Gas2	*1.19*	10.07	*1.78*	0.0177
101344_at	NM_007627	Cholecystokinin B receptor	Cckbr	*1.04*	*1.44*	2.34	0.0177
95363_at	NM_008504	Granzyme M (lymphocyte met-ase 1)	Gzmm	—	3.16	4.82	0.0180
98560_at	NM_028870	Clathrin, light polypeptide (Lcb)	Cltb	*1.01*	2.43	3.71	0.0180
92904_at	NM_007548	PR domain containing 1, with ZNF domain	Prdm1	*1.13*	*1.40*	2.71	0.0300
102234_at	NM_024461	RIKEN cDNA *1810037I17* gene	1810037I17Rik	1.89	1.78	2.62	0.0314
92293_at	NM_176930	Neuronal cell adhesion molecule	Nrcam	*1.16*	*1.62*	2.27	0.0316
99111_at	NM_009191	Suppressor of K^+ transport defect 3	Skd3	*1.03*	2.25	2.23	0.0347
93973_at	NM_133916	Eukaryotic translation initiation factor 3, subunit 9 (eta)	Eif3s9	*−1.08*	*1.41*	2.24	0.0370
97206_at	NM_016907	Serine protease inhibitor, Kunitz type 1	Spint1	—	2.28	—	0.0380
98338_at	NM_010134	Engrailed 2	En2	*−1.02*	*1.04*	2.72	0.0426
92415_at	NM_009404	Tumor necrosis factor (ligand) superfamily, member 9	Tnfsf9	*1.05*	2.65	—	0.0479
101190_at	NM_008639	Melatonin receptor 1A	Mtnr1a	*1.18*	2.33	—	0.0566
96911_at	XM_282613	Guanine nucleotide binding protein, beta 2	Gnb2	*−1.01*	*1.30*	2.22	0.0566
160705_at	NM_007709	Cbp/p300-interacting transactivator w/E/D-rich carboxy-terminal dom 1	Cited1	*1.08*	2.34	*1.55*	0.0566
98424_at	NM_011204	Protein tyrosine phosphatase, non-receptor type 13	Ptpn13	*1.20*	*1.54*	2.24	0.0647
162206_f_at	NM_007707	Suppressor of cytokine signaling 3	Socs3	*1.14*	*1.62*	2.44	0.0650
96862_at	NM_134054	RIKEN cDNA *1110002B05* gene	1110002B05Rik	*1.24*	2.28	2.43	0.0670
94256_at	NM_013885	Chloride intracellular channel 4 (mitochondrial)	Clic4	*1.22*	*1.65*	2.28	0.0690
103033_at	NM_009780	Complement component 4 (within H-2S)	C4	*1.05*	*−1.11*	2.69	0.0700
101706_at	NM_009918	Cyclic nucleotide gated channel alpha 3	Cnga3	—	2.24	2.60	0.0780
93269_at	NM_025374	Glyoxalase 1	Glo1	*1.00*	*1.41*	2.15	0.0900
93731_at	NM_012056	FK506 binding protein 9	Fkbp9	*−1.19*	*1.48*	4.49	0.0910
96518_at	XM_109956	KIBRA protein	Kibra**	*1.09*	2.12	2.29	0.0934
103456_at	AW322500	Expressed sequence AW322500	AW322500	*−1.18*	2.69	2.34	0.1190
92232_at	NM_007707	Suppressor of cytokine signaling 3	Socs3**	*1.06*	*1.64*	2.37	0.1200
104374_at	NM_009252	Serine (or cysteine) proteinase inhibitor, clade A, member 3N	Serpina3n	—	—	2.82	0.1251
104564_at	NM_009130	Secretogranin III	Scg3	*1.13*	1.93	2.49	0.1251
103241_at	NM_153534	Adenylate cyclase 2	Adcy2	*1.34*	1.92	1.95	0.1350
94393_r_at	NM_019423	ELOVL family member 2, elongation of long chain fatty acids (yeast)	Elovl2	*1.33*	2.82	3.09	0.1370
92534_at	NM_010276	GTP binding protein (gene overexpressed in skeletal muscle)	Gem	*1.16*	*1.42*	2.82	0.1535
100026_at	NM_007532	Branched chain aminotransferase 1, cytosolic	Bcat1	*1.01*	*1.38*	1.96	0.1540
99972_at	NM_009414	Tryptophan hydroxylase 1	Tph1	—	*1.49*	2.15	0.1590
95105_at	NM_025933	RIKEN cDNA *2010110M21* gene	2010110M21Rik	*1.01*	*1.71*	2.06	0.1670
97722_at	NM_025965	Signal sequence receptor, alpha	Ssr1	2.17	2.03	1.96	0.1770
93268_at	NM_025374	Glyoxalase 1	Glo1**	*1.13*	*1.42*	2.34	0.2070
93669_f_at	NM_009234	SRY-box containing gene 11	Sox11	3.41	*1.75*	—	0.2220
94872_at	NM_020561	Acid sphingomyelinase-like phosphodiesterase 3a	Asml3a-pending	*1.04*	1.89	1.94	0.2220
99014_at	XM_133641	Amyloid beta (A4) precursor protein-binding, family B, member 1	Apbb1	*−1.01*	*1.58*	1.88	0.2550
93412_at	NM_010045	Duffy blood group	Dfy	*1.10*	*1.35*	1.94	0.2570
97124_at	NM_008016	Fibroblast growth factor inducible 15	Fin15	*1.16*	*1.90*	2.32	0.2940
104104_at	NM_030237	Spermatogenic Zip 1	Spz1-pending	*−1.20*	*1.20*	2.41	0.3120
94733_at	NM_008830	ATP-binding cassette, sub-family B (MDR/TAP), member 4	Abcb4	*1.05*	*1.37*	1.77	0.3140
104761_at	XM_132228	Anthrax toxin receptor	Antxr2	*1.13*	*1.18*	2.36	0.3275
101044_at	NM_008525	Aminolevulinate, delta-, dehydratase	Alad	*1.27*	1.90	1.82	0.3328

Continued

Table 1. *Continued*

Probeset	Accession no.	Gene description	Name	P2 AFC	P10 AFC	2M AFC	*P*-value
99623_s_at	NM_019498	Olfactomedin 1	Olfm1	*1.05*	*1.47*	2.18	0.3410
98544_at	NM_008193	Guanylate kinase 1	Guk1	*1.02*	*−1.01*	1.88	0.3819
98111_at	NM_013559	Heat shock protein 105	Hsp105	*1.18*	*1.06*	2.33	0.4600
92770_at	XM_192936	S100 calcium binding protein A6 (calcyclin)	S100a6	*1.13*	*1.09*	2.13	0.4870
101861_at	NM_011360	Sarcoglycan, epsilon	Sgce	*−1.03*	*1.38*	1.70	0.4890
104388_at	NM_011338	Chemokine (C–C motif) ligand 9	Ccl9	—	—	2.12	0.5800
160937_at	NM_016669	Crystallin, mu	Crym	*1.00*	*1.23*	1.99	0.6290
93354_at	NM_007469	Apolipoprotein C-I	Apoc1	—	1.82	—	0.6778
98005_at	NM_008862	Protein kinase inhibitor, alpha	Pkia	*1.07*	*1.25*	2.14	0.6870
101191_at	NM_007873	Double C2, beta	Doc2b	*−1.01*	*−1.04*	1.95	0.7286
104469_at	NM_010329	Glycoprotein 38	Gp38	*1.26*	*1.23*	2.10	0.7560
94258_at	NM_007486	Rho, GDP dissociation inhibitor (GDI) beta	Arhgdib	*1.09*	*1.08*	1.86	0.7801
160414_at	NM_024249	RIKEN cDNA *1810073N04* gene	1810073N04Rik	*1.01*	1.84	*1.36*	0.8697
95397_at	XM_196081	RIKEN cDNA *D430019H16* gene	D430019H16Rik	*1.04*	1.73	*1.63*	0.9320
93496_at	NM_134255	ELOVL family member 5, elongation of long chain fatty acids (yeast)	Elovl5	*−1.02*	*1.26*	1.96	0.9810

Differentially expressed genes are listed based on statistical ranking (FDRCI *P*-values) and all are shown with a *P*-value < 1 based on a 1.5 minfc MGU74Av2 probeset IDs and corresponding GenBank accession numbers (RefSeq if available) are given. Where multiple probesets correspond to a single gene, the additional probesets are indicated by asterisks and italicized text. AFC in expression in Nrl relative to wild-type is shown for the three time-points analyzed, P2, P10 and 2 months (2M) after signal quantification and normalization by RMA. Dashes indicate that gene expression was reported as absent (by MAS5) on all eight GeneChips for the given time-point (i.e. wild-type and $Nrl^{-/-}$). Italicized numbers indicate a non-significant AFC as determined by statistical analysis (*P*-value = 1). The lowest *P*-values are given for the three time-points measured for each of the gene probesets.

addition to a level of statistical significance. Although the highly differentially expressed genes are near the top of the lists as expected, the order is based on both the AFC and the variability of the signal data across the GeneChips. For this reason, probesets displaying a relatively high AFC for a given time-point may still be reported as non-significant [e.g. Nt5e (down-regulated) and Fin15 (up-regulated) at P10 in Table 1]. After removing probesets that belong to the same gene and show similar gene expression profile, a non-redundant set comprising 78 down-regulated and 83 up-regulated genes is obtained. Almost 90% of these genes are categorized as 'known', whereas 18 are novel sequences that are represented currently only in expressed sequence tag (EST) or genomic sequence databases.

Validation by quantitative real-time PCR

Fifty-four different gene/time-point values spanning a broad spectrum of AFC and FDRCI rankings were examined by quantitative real-time PCR (Q-PCR) (Table 2). There is a good correlation ($R^2 = 0.91$, data not shown) between AFC reported by microarray and by Q-PCR. Underestimation of the relative degree of fold-change in microarray data is likely due to background noise and limited sensitivity that restricts the dynamic range of this hybridization-based technique. Only three genes (*Gas5*, *Sox11* and *1110002B05Rik*) showed disagreement between the two methods (94% validation rate). The discrepancy could be due to the existence of multiple isoforms, which have been identified for these genes. The importance of validation is evident, not only for identifying possible false positives but also for determining the relative fold-change in transcripts (i.e. biological change) compared with the AFC reported by microarray. For example, Guca1a and Kibra are both predicted to be moderately up-regulated (5.6 and 6.0, respectively) in the $Nrl^{-/-}$ retina; however, Guca1a is shown to be up-regulated 5.5-fold by Q-PCR (same as microarray) but Kibra 26-fold (5-fold underestimate by microarray). Similar examples are evident amongst the down-regulated genes. Q-PCR analysis using additional retinal samples for six of the genes revealed similar AFCs (data not shown).

Hierarchical clustering and functional annotation

Relative expression profiling across multiple developmental time-points can provide information on the potential role of a given gene in the context of known biological events occurring within that time frame. Comparison of relative profiles can allow clustering of genes into groups that show similar patterns of behavior. To compare expression patterns between all 161 differentially expressed genes, the average signals from the four replicate GeneChips were first normalized to z-scores, and then run through a hierarchical clustering algorithm. Ten major clusters were identified by visual inspection, and Gene Ontology was used to assign functional annotation of 101 genes (62%) (Fig. 1).

Cluster I contains genes that display a bimodal (peaks at P2 and 2 month) or constant pattern of expression in wild-type, but show significantly decreased expression at P10 or 2 months of age in the $Nrl^{-/-}$ retina. Cluster II contains three γ-crystallin genes (E, D and F); for these, the peak expression is in the wild-type adult retina, but in the $Nrl^{-/-}$ retina there is increased expression at P2 and P10 but a significant decrease at 2 months. Although these genes show AFCs >2-fold at P10, none of these is considered statistically significant (Table 1). This may be due to the signal noise associated with the high degree of sequence identity between different crystallins. Q-PCR confirmed the decreased expression of Crygd and

Table 2. Real-time Q-PCR validation

Name	AFC	Q-PCR	*P*-value
Down-regulated genes			
Dp1l1	−15.9	−43.3	0.0001
Pde6b	−25.0	−52.7	0.0002
Rho	−41.3	−1604.0	0.0003
Cnga1	−13.6	−406.4	0.0004
Gnb1	−8.1	−78.3	0.0004
Gas5	−6.3	−1.8	0.0008
Aqp1	−7.8	−52.3	0.0011
Mef2c	−4.2	−4.6	0.0029
Gnat1	−216.4	−3494.4	0.0046
Cdr2	−5.5	−7.0	0.0080
Pdir-pending	−2.7	−14.3	0.0120
Pde6a	−3.0	−13.3	0.0160
Zfp36l2	−3.7	−7.7	0.0197
Rom1	−3.3	−5.7	0.0280
2900026H06Rik*	−3.2	−4.7	0.0340
Wisp1	−3.3	−32.7	0.0479
Tnfaip3	−4.5	−7.5	0.0580
D6Wsu176e	−3.3	−9.2	0.0650
D1Ertd622e	−2.5	−7.7	0.0934
Abca4	−2.2	−6.6	0.1081
Mpdz	−2.6	−7.9	0.1084
0610012A05Rik	−2.7	−3.6	0.2140
Mbnl1*	−2.0	−2.2	0.2530
Lmo1	−1.9	−9.6	0.2940
Drd4*	−4.5	−12.7	0.3410
Crygf	−3.5	−4.8	0.4940
Crygd	−3.2	−6.5	0.7652
Up-regulated genes			
Clca3	14.9	44.2	0.0003
Opn1sw	9.4	23.1	0.0004
Casp7	6.4	10.7	0.0017
Gnat2	7.6	15.3	0.0029
Txndc5	2.7	7.8	0.0047
Fabp7	7.3	49.1	0.0065
Epha8*	2.6	10.1	0.0080
Inhbb*	2.8	9.5	0.0080
Rxrg	2.9	8.9	0.0108
Guca1a*	5.6	5.5	0.0115
Kibra	6.0	26.0	0.0120
Gnb3	5.3	8.2	0.0130
Sall3	2.6	2.4	0.0130
Camk2b	3.1	15.6	0.0166
Gas2*	10.1	52.8	0.0177
Sall3*	3.5	20.8	0.0180
Gzmm	4.8	2.5	0.0180
Prdm1	2.7	7.6	0.0300
1810037I17Rik	2.6	2.1	0.0314
En2	2.7	31.3	0.0426
Socs3	2.4	19.7	0.0650
Serpina3n	2.8	3.2	0.1251
Elovl2	3.1	5.1	0.1370
1110002B05Rik	2.4	1.2	0.1880
Sox11**	3.4	−2.0	0.2220
Antxr2	2.4	7.0	0.3275
Olfm1	2.2	2.0	0.3410

AFC is based on the microarray data with corresponding FDRCI *P*-value. Relative fold-change based on Q-PCR is shown. All measurements were on adult (2M) retina except where indicated (**P2, *P10). Underlined values indicate genes for which there are significant discrepancies between the two methods [i.e. no significant change reported by Q-PCR (<2-fold) or direction of change is in disagreement with microarray data].

Crygf at 2 months (Table 2). Crystallins are expressed in neural retina and may play a role in stress response (33). For the genes of Cluster V, their expression peaks at P10 but then decreases (though still detectable) in the wild-type adult retina. In the $Nrl^{-/-}$ retina, the peak expression may still be at P10, but is reduced for all these genes, suggesting a potential role in differentiation, as indicated for Ndr1, Ndrl and Lmo1. Cluster VI contains only two ESTs that are expressed across all three time-points but are down-regulated in the $Nrl^{-/-}$ retina.

Almost 80% of genes showing decreased expression in the $Nrl^{-/-}$ retina belong to clusters III and IV. These genes demonstrate an increasing (relative) level of expression, reaching peak expression by P10 (cluster III) or 2 months (cluster IV) in wild-type, suggesting a role in the mature retina/photoreceptors. In the $Nrl^{-/-}$ retina, these genes are down-regulated showing, typically, only a moderate (or no) increase in expression at later time-points. Genes of these clusters are strong candidates for direct positive regulation by Nrl and include Rho, Pde6b and Pde6a (known targets of Nrl) as well as Gnat1 and Gnb1.

The genes showing higher expression in the $Nrl^{-/-}$ retina can be organized into four major clusters. The genes of the largest cluster VIII show an increase in expression at P10 or 2 months in the $Nrl^{-/-}$ retina relative to wild-type. As anticipated, this includes genes encoding proteins with a role in cone-mediated visual function (e.g. Opn1sw and Gnat2). Expression of cluster VII genes peaks at P2 in wild-type, suggesting a primary role in early development, but in the $Nrl^{-/-}$ retina they show elevated expression peaking at P10 or 2 months. Their sustained high expression in the adult retina may be indicative of an aberrant reactivation of gene expression, possibly related to stress, cell death or reactive gliosis. Cluster IX genes show an elevated differential expression (and peak) in the $Nrl^{-/-}$ retina, primarily at P10, and may play a role in cone differentiation. Of the 14 genes in this cluster, six are associated with signaling, development or cell cycle/growth. Cluster X includes genes showing peak expression at P2 in wild-type but the expression declines (often rapidly) by P10 or 2 months, suggesting a primary role in early development. In the $Nrl^{-/-}$ retina, the expression profile is similar but the expression is elevated and maintained for a longer period.

Direct targets of Nrl identified by ChIP

We hypothesized that targets of Nrl will be enriched among the genes exhibiting reduced expression in the $Nrl^{-/-}$ retina. Hence, we examined the enrichment of the promoter regions that include a potential AP-1 like or Nrl-response element (NRE) of 'candidate Nrl targets' by ChIP with a polyclonal anti-Nrl antibody (8) using the wild-type mouse retina. Twenty different gene promoters were assayed by PCR amplification; of these, 18 (90%) showed enrichment in the antibody fractions (Nrl-ChIP) over the no antibody control (Fig. 2), demonstrating *in vivo* promoter occupancy by Nrl. The positive target promoters included three genes (*Rho*, *Pde6b* and *Pde6a*) that are modulated by Nrl. The promoters of other photoreceptor genes (such as *Cnga1*, *Gnat1*, *Gnb1*, *Rom1* and *Pdc*) were also enriched. In addition, a few widely expressed genes, such as *Aqp1* (water channel) and adiponectin receptor 1 (*AdipoR1*), appear to be the target of Nrl

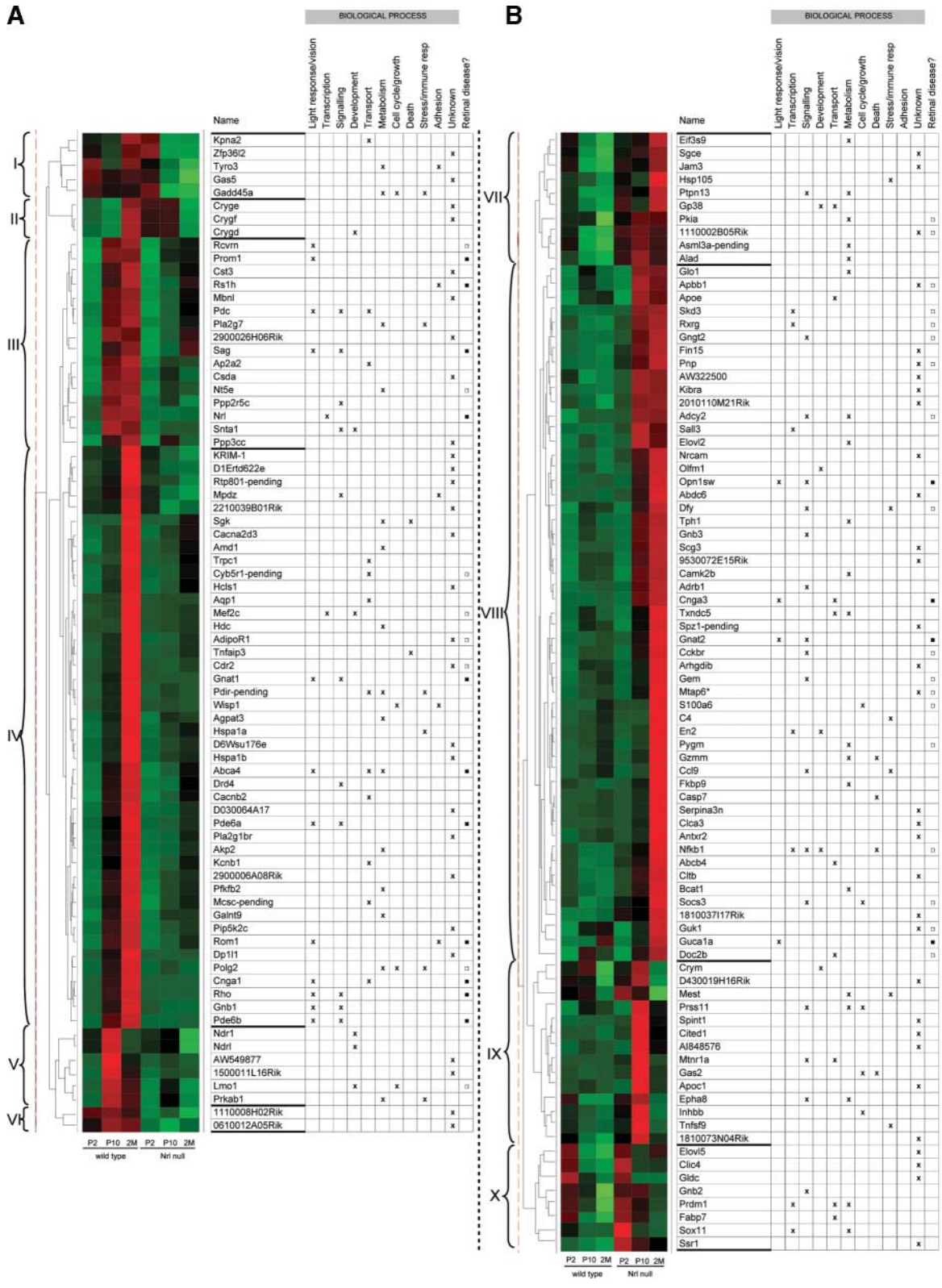

Figure 1. Hierarchical clustering and functional annotation. Clustering of differentially expressed genes based on normalized average signals (z-scores). Bright green boxes indicate lowest signal with increasing values indicated by darkening color towards bright red, representing peak signal. The set of 161 non-redundant genes are divided, based on similarity of profiles, into 10 clusters. (**A**) Down-regulated genes are in groups I–VI and (**B**) up-regulated in groups VII–X. Functional annotation is based on defined biological processes assigned by the Gene Ontology (GO) consortium. Though listed as having no defined function, Mtap6 (indicated by an asterisk) is associated with microtubules and has a presumed role in synaptic plasticity and function. The far right column indicates whether the gene is known to be associated with (black square) or is a candidate for (empty square) retinal disease (see Table 3 also).

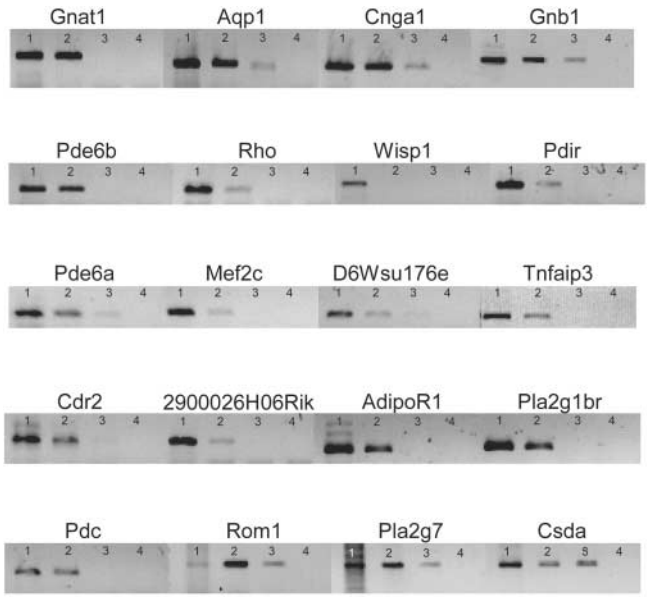

Figure 2. ChIP analysis. PCR products are shown for 20 different gene promoters in which the most proximal putative AP-1/NRE-like site was assayed. Each set includes the input genomic DNA as positive control (lane 1), chromatin DNA fraction immunoprecipitated with anti-NRL antibody (lane 2), chromatin DNA obtained without the antibody (background control; lane 3) and water (negative control; lane 4). Enrichment (greater amount of product) with antibody IP over background control (no Ab) indicates the *in vivo* occupancy of a sequence element within the amplified region by Nrl. All assayed gene promoters showed enrichment, except Wisp1 (inconclusive) and Csda (negative). Direct regulation of Rho and Pde6b by Nrl (at these sites) has been demonstrated previously, and as such these are positive controls for the ChIP protocol.

regulation in mature rods. It should be noted that although only down-regulated genes were analyzed by ChIP, Nrl might negatively regulate (i.e. repress) the expression of cone-specific genes, much akin to the predicted role of Nr2e3 (21).

Identification of retinal disease candidate genes

Many genes showing photoreceptor-enriched expression are associated with retinal disease; these encode diverse functions, including phototransduction (e.g. rhodopsin), transcriptional regulation (e.g. *Crx* and *Nrl*), outer segment structure (e.g. *Rom1* and *Prom1*) or maintenance of the extracellular matrix (e.g. *Rs1h*). Expression profiling of a mouse model with retinal degeneration ($Rho^{-/-}$) was utilized previously to identify a retinitis pigmentosa disease gene (*RP10*), inosine monophosphate dehydrogenase type 1 (IMPDH1) (34), which was not an obvious candidate due to its ubiquitous expression and role in guanosine nucleotide biosynthesis. We, therefore, determined the chromosomal location of genes that are expressed differentially in the $Nrl^{-/-}$ retina using *in silico* methods. On the basis of the map position of the human homolog, 41 of the differentially expressed genes (25%) have been associated previously with or are candidates for retinal diseases (Table 3). A few of these (e.g. *Mef2c*, *Nt5e* and *Cdr2*) were also identified in the $Rho^{-/-}$ gene profiling study (34), providing further evidence of their rod-preferred expression. Up-regulated genes that are candidates for macular or cone associated diseases include *S100A6*, *RXRG*, *ADCY2*, *NP* and *SOCS3*, whereas down-regulated genes that map to the region of rod associated disease loci (such as RP) include *NT5E* and *CDR2*.

Analysis of differentially expressed genes

Light response and vision. The genes displaying restricted expression to rods or cones show the most dramatic changes in expression. For the rods, these include genes encoding rod-specific phototransduction proteins such as rhodopsin (Rho), cGMP phosphodiesterase subunits (Pde6a and b), rod transducin subunits (Gnat1 and Gnb1) and the cyclic nucleotide gated channel subunit (Cnga1). By Q-PCR, transcripts of these genes are virtually undetectable in the $Nrl^{-/-}$ retina with expression typically $<1\%$ of wild-type. Modest expression of Pde6a ($\sim 7\%$) and Pde6b ($\sim 2\%$) in the adult $Nrl^{-/-}$ retina can be attributed to their expression in non-photoreceptor neurons, as observed for Pde6a (35). Genes encoding cone phototransduction proteins, such as the photopigment S-opsin (Opn1sw), cone transducin subunits (Gnat2, Gnb3 and Gngt2) and the cyclic nucleotide gated channel subunit (Cnga3), show dramatically higher expression in the $Nrl^{-/-}$ retina. A number of genes that are expressed in both photoreceptor subtypes show varying degrees of expression change, which may reflect a moderate quantitative bias towards one class (or expression in multiple cell types). These include guanylate cyclase activator 1a (Guca1a or Gcap1), recoverin (Rcvrn), prominin 1 (Prom1), phosducin (Pdc), retinal S-antigen (Sag), retinal outer segment membrane protein (Rom1) and an ATP-binding cassette (ABC) transporter (Abca4). Guca1a displays a 5.5-fold increase in expression in the $Nrl^{-/-}$ retina suggesting preferential expression in cones. Notably, although expressed in both rods and cones, mutations in this gene are primarily associated with cone or cone–rod dystrophies (36,37). Other down-regulated genes may indicate their preferential expression in rods.

Gene regulation, differentiation and development. Transcription factors and signaling molecules that are expressed differentially in the $Nrl^{-/-}$ retina may provide insights into the regulatory networks associated with photoreceptor development and/or function. Q-PCR analysis of E14–P21 retina for the cone photopigment Opn1sw (S-opsin) showed that the increase in its expression occurred at P6.5 in the $Nrl^{-/-}$ retina (Fig. 3). This second-wave of cone differentiation likely corresponds to the post-mitotic photoreceptors that are normally destined to become rods. Therefore, it is predicted that genes associated with rod or cone differentiation would be down- or up-regulated, respectively, at this time-point. The expression of MADS-box containing myocyte enhancer factor 2c (Mef2c) (38,39) is reduced in the matured $Nrl^{-/-}$ retina to 20% of the wild-type levels. Zfp36l2 (a C3H-type zinc finger protein) is down-regulated $\sim$8-fold in the $Nrl^{-/-}$ retina. A significant decrease in expression of LIM domain only 1 (Lmo1), a developmentally associated transcription factor, is observed in the adult retina (10-fold by Q-PCR) suggesting its role in mature rods. Similar profiles are also

Table 3. Disease association or candidacy for differentially expressed genes

Mouse gene description	AFC			Human homolog		Disease
	P2	P10	2M	Name	Location	
Known disease genes						
Guanine nucleotide binding protein, alpha transducing 2	1.5	7.2	7.6	GNAT2	1p13.1	Recessive achromatopsia (ACHM4)
ATP-binding cassette, sub-family A (ABC1), member 4	−1.4	−2.8	−2.2	ABCA4	1p22.1-p21	Recessive Stargardt (STGD1)/recessive MD/ recessive RP (RP19)/recessive fundus flavimaculatus/recessive cone-rod dystrophy
Cyclic nucleotide gated channel alpha 3	—	2.2	2.6	CNGA3	2q11.2	Recessive achromatopsia (ACHM2)
Retinal S-antigen	−5.1	−4.1	−1.2	SAG	2q37.1	Recessive Oguchi disease / recessive RP
Guanine nucleotide binding protein, alpha transducing 1	−1.2	−55.6	−216.4	GNAT1	3p21	Dominant congenital stationary night blindness
Rhodopsin	—	−24.8	−41.3	RHO	3q21-24	Dominant RP / recessive RP / dominant congenital stationary night blindness
Cyclic nucleotide gated channel alpha 1	—	−7.3	−13.6	CNGA1	4p12-cen	Recessive RP
Prominin 1	1.0	−1.9	−1.6	PROM1	4p15.33	Recessive retinal degeneration
Phosphodiesterase 6B, cGMP, rod receptor, beta polypeptide	−2.3	−37.3	−25.0	PDE6B	4p16.3	Recessive RP / dominant congenital stationary night blindness
Phosphodiesterase 6A, cGMP-specific, rod, alpha	—	−2.1	−3.0	PDE6A	5q31.2-q34	Recessive RP
Guanylate cyclase activator 1a	−1.2	5.6	1.4	GUCA1A	6p21.1	Dominant cone dystrophy
Opsin 1 (cone pigments), short-wave-sensitive	1.3	8.4	9.4	OPN1SW	7q31.3-q32	Dominant tritanopia
Retinal outer segment membrane protein 1	−2.2	−5.3	−3.3	ROM1	11q13	Dominant RP / digenic RP (with RDS)
Neural retina leucine zipper gene	—	−2.6	−2.5	NRL	14q11.1-q11.2	Dominant RP (RP27)
Retinoschisis 1 homolog (human)	—	−2.7	−1.6	RS1	Xp22.2-p22.1	Retinoschisis (XLRS1)
Candidate disease genes						
S100 calcium binding protein A6 (calcyclin)	1.1	1.1	2.1	S100A6	1q21	
Duffy blood group	1.1	1.3	1.9	FY	1q21-q22	Recessive cone-rod dystrophy (CORD8)
Retinoid X receptor gamma	−1.0	2.5	2.9	RXRG	1q22-q23	
Adiponectin receptor 1	−1.2	−1.4	−2.7	ADIPOR1	1q32.1	Recessive ataxia, posterior column with RP (AXPC1)
Cytochrome b5 reductase 1 (B5R.1)	1.1	−1.4	−2.0	CYB5R1	1q32.1	
Guanylate kinase 1	1.0	−1.0	1.9	GUK1	1q32-q41	
Nuclear factor of kappa light chain gene enhancer in B-cells 1, p105	1.1	1.8	3.1	NFKB1	4q24	Wolfram syndrome (WFS2)
Adenylate cyclase 2	1.3	1.9	2.0	ADCY2	5p15.3	Dominant macular dystrophy (MCDR3)
Myocyte enhancer factor 2C	–	–	−4.2	MEF2C	5q14	Dominant Wagner disease (WGN1) and erosive vitreoretinopathy (ERVR)
5′ nucleotidase, ecto	1.1	−2.1	−2.7	NT5E	6q14-q21	Recessive RP (RP25)
GTP binding protein (gene overexpressed in skeletal muscle)	1.2	1.4	2.8	GEM	8q13-q21	
Protein kinase inhibitor, alpha	1.1	1.2	2.1	PKIA	8q21.11	Recessive optic atrophy (ROA1)
LIM domain only 1	−1.2	−1.5	−1.9	LMO1	11p15	
Amyloid beta (A4) precursor protein-binding, family B, member 1	−1.0	1.6	1.9	APBB1	11p15	Dominant atrophia areata; dominant chorioretinal degeneration, helicoid (AA)
Cholecystokinin B receptor	1.0	1.4	2.3	CCKBR	11p15.4	
Muscle glycogen phosphorylase	—	1.2	4.3	PYGM	11q13.1	
Microtubule-associated protein 6	−1.1	1.5	3.0	MAP6*	11q13.3	Dominant neovascular inflammatory vitreoretinopathy (VRNI)
Suppressor of K^+ transport defect 3	1.0	2.2	2.2	SKD3	11q13.3	
RIKEN cDNA 1110002B05 gene	1.2	2.3	2.4	C14orf147*	14q13.1	Dominant MD, North Carolina-like with progressive sensorineural hearing loss (MCDR4) recessive rod monochromacy or achromatopsia (ACHM1)
Purine-nucleoside phosphorylase	1.5	3.0	4.2	NP	14q13.1	
Cerebellar degeneration-related 2	−1.1	−3.0	−5.5	CDR2	16p12.3	Recessive RP (RP22)
Recoverin	—	−2.4	−2.1	RCV1	17p13.1	
Double C2, beta	−1.0	−1.0	2.0	DOC2B	17p13.3	Dominant central areolar choroidal dystrophy (CACD)
Polymerase (DNA directed), gamma 2, accessory subunit	−1.0	−1.7	−3.6	POLG2	17q	
Guanine nucleotide binding protein, gamma transducing activity pp 2	1.1	6.2	7.9	GNGT2	17q21	Cone rod dystrophy (CORD4)
Suppressor of cytokine signaling 3	1.1	1.6	2.4	SOCS3	17q25.3	

Differentially expressed genes that are known to be associated with retinal diseases or candidate genes that map to disease intervals are shown. AFC is shown as given in Table 1. *Indicates that gene is the likely human homolog but is not, as yet, definitively assigned as such (based on LocusLink).

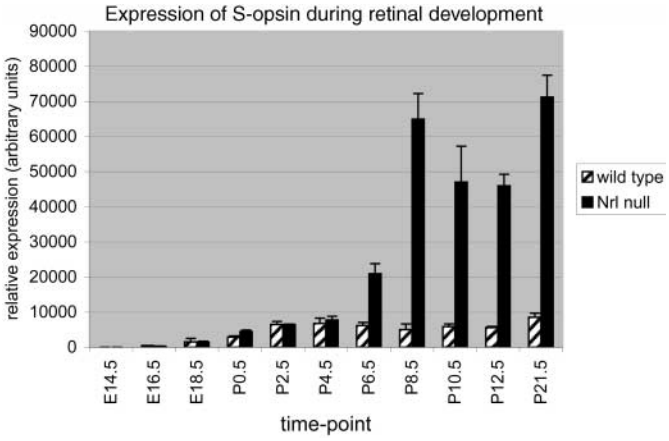

Figure 3. Temporal expression of S-opsin in the wild-type and $Nrl^{-/-}$ retina. The profile of relative expression of S-opsin determined by Q-PCR on the developing mouse retinas is shown after normalization to Hprt. Error bars indicate s.e.m.

observed for N-myc downstream regulated 1 (Ndr1) and Ndr-like (Ndrl).

A number of genes encoding transcription regulatory proteins are up-regulated in the $Nrl^{-/-}$ retina. Retinoid X receptor gamma (Rxrg), localized to cones in the adult retina (40) and shown to be induced by retinoic acid (RA) (41), shows 9-fold higher expression in the $Nrl^{-/-}$ retina. Rxrg maps to the region of cone-dystrophy locus CORD8 (Table 3) and is an excellent candidate for this disease. Sal-like 3 (Sall3), a C2H2 zinc finger transcription factor, is required for terminal differentiation of photoreceptors in *Drosophila* (42); its augmented expression is therefore of considerable interest. Validation by Q-PCR, which detects two of the six alternative transcripts, reveals that Sall3 is highly differentially expressed at P10 (20-fold) but is only moderately increased at 2 months (2-fold), suggesting a potential role in cone differentiation. Engrailed-2 (En2), a homeobox transcription factor, shows sustained expression in the mature wild-type retina but in $Nrl^{-/-}$ retina it is highly elevated (30-fold increase). The positive regulatory domain zinc finger protein, Prdm1, shows elevated expression (8-fold) in the matured $Nrl^{-/-}$ retina. It is expressed earlier in the wild-type retina and is undetectable in the adult.

Apoptosis and stress response

Several genes encoding proteins associated with stress response or apoptosis exhibit decreased expression in the $Nrl^{-/-}$ retina; these include the chaperone heat shock proteins Hsp70.3 (Hspa1a) and Hsp70.1 (Hspa1b). Serum/glucocorticoid regulated kinase (Sgk), which shows peak expression in the adult retina and is down-regulated in the $Nrl^{-/-}$ retina, is shown to be anti-apoptotic and induced in response to multiple forms of stress in epithelial cells (43). Tumor necrosis factor alpha induced protein 3 (Tnfaip3), which inhibits NF-kappa B (Nfkb1) (44), has been associated with light-induced photoreceptor degeneration (45). Tnfaip3 is first detected at P10, and its expression peaks at 2 months. In contrast, Nfkb1 expression is relatively constant in the wild-type retina but exhibits a moderate peak at P2. In the $Nrl^{-/-}$ retina, Tnfaip3 is down-regulated 8-fold, whereas its inhibitory target, Nfkb1, is up-regulated. This observation, may at least in part, provide clues to the mechanism through which stress response and cell death may be mediated in the $Nrl^{-/-}$ retina during late stages (unpublished data). Caspase-7, which is detected in the wild-type retina during development, is the only caspase showing elevated (10-fold) expression in the adult $Nrl^{-/-}$ retina.

Calcium homeostasis and retinal function

During the recovery of light response in photoreceptors, cGMP is regulated by cytoplasmic Ca^{2+} via Guca1a (or Gcap1). Both Guca1a and rod arrestin (Sag) are associated with retinal diseases and are expressed differentially in the $Nrl^{-/-}$ retina. Calcium/calmodulin-dependent kinase II beta (Camk2b) is up-regulated (15-fold) in the $Nrl^{-/-}$ retina. Calcyclin (S100a6) is expressed highly in neurons (46) and shows elevated levels in the $Nrl^{-/-}$ retina. The human homolog of this gene maps to a cone–rod dystrophy locus (CORD8). S100a6 is regulated by NF-kappaB (47), which is also augmented in the $Nrl^{-/-}$ retina. Two calcium channels genes *Trpc1* and *Cacnb2* are down-regulated in the $Nrl^{-/-}$ retina. Syntrophin acidic 1 (Snta1) is a component of the dystrophin glycoprotein complex (DGC) which may play a significant structural and signaling role (neurotransmission) in the retina (48). Mutations of dystrophin or disruption of the DGC may account for scotopic (rod response) defects in patients with Duchenne muscular dystrophy (49), consistent with rod-enrichment of Snta1 and its down-regulation in the $Nrl^{-/-}$ retina.

Melatonin signaling. Retinal melatonin, acts as a local neuromodulator through the melatonin receptors, which then may control the release of dopamine (50). Three genes of the melatonin pathway, tryptophan hydroxylase (Tph1), dopamine receptor 4 (Drd4) and melatonin receptor 1a (Mtnr1a), are expressed differentially in the $Nrl^{-/-}$ retina. Tph1 is the first enzyme in the biosynthetic pathways of melatonin in the photoreceptors and is believed to be synthesized primarily in the cones (51), consistent with its up-regulation in the $Nrl^{-/-}$ retina. The melatonin receptor 1a, which normally shows peak expression around P2–P4, is highly elevated in the $Nrl^{-/-}$ retina, and peaks at P8 before rapidly decreasing in expression. The dopamine receptor Drd4, which plays a role in regulating cAMP metabolism, is not highly expressed until P10–P12 in the wild-type retina (52), but is down-regulated to $<10\%$ of the wild-type levels in the P10 $Nrl^{-/-}$ retina, indicating a role in rods.

Novel functions and novel genes

Although a majority of the differentially expressed genes have a defined function, in many cases their specific role in the retina or their possible bias towards rods or cones is not understood. Deleted in polyposis 1-like 1 (*Dp1l1*) is the top FDRCI ranked down-regulated gene and is expressed at $<3\%$ of the wild-type levels. It shows peak expression in the adult retina and is detected in the outer nuclear layer (data not shown) but its function is unknown. A function can be inferred but

is not known for calcium activated chloride channel 3 (Clca3), which is up-regulated 44-fold in the $Nrl^{-/-}$ retina. Kibra is a novel WW-domain containing protein expressed primarily in brain and kidney (53) and is up-regulated 26-fold in the $Nrl^{-/-}$ retina. In addition, 18 of the differentially expressed genes identified by microarray analysis match only ESTs. These novel genes could provide new leads for elucidating retinal development and function.

DISCUSSION

Expression profiling and data mining

Appropriate microarray design and data analysis are essential for extracting meaningful results in genome-wide expression profiling studies (54). We utilized RMA for normalization (29,32) and chose an AFC cut-off of 1.5. A new two-stage gene filtering procedure (55) was applied that controls both FDR and minfc levels. This procedure is based on construction of a set of simultaneous FDRCI on the temporal fold-changes of each gene. Genes having at least one confidence interval that covers a range of fold-changes larger than the specified AFC cut-off, which we call minfc, are declared significant at the specified FDRCI level. As FDRCI is more stringent than FDR, the associated significance levels are generally not as high as those of the FDR procedure. For each minfc level studied, the two-stage procedure was used to generate a list of genes ranked according to decreasing FDRCI significance or, equivalently, increasing FDRCI *P*-value. For an AFC cut-off of 1.5, the complete ranked list, excluding probesets having FDRCI *P*-values >0.99, consisted of 173 probesets. Of the 54 data points tested by Q-PCR, 51 (94%) were verified. If the minfc is reduced to 1.25, the probeset list is expanded to over 300 probesets (see Supplementary Material, Table A). These additional genes may display a reduced validation rate by Q-PCR but add to cluster analysis and pathway construction based on the microarray data. Replicate experiments and statistical analysis are critical for extracting such probesets.

Temporal profiling and clustering analysis add a new dimension for predicting the functional role, possible interactions and regulatory relationships that may exist amongst the genes that are being analyzed. Our studies should identify the genes that are presumably associated with photoreceptor development (P2), terminal differentiation (P10) and function (2 month). Although our data are based on a mixed cell population (whole retina), the generated profiles are dominated by photoreceptors (about 70% of total cells) and can direct future studies to prioritize candidate genes of interest for positional cloning or functional analysis. Of particular interest are the differentially expressed genes encoding proteins associated with visual process, transcriptional regulation, signal transduction and development, as they may provide insights into the regulatory networks and signaling pathways underlying the differences between rods and cones.

Genes encoding metabolism-related proteins represented the single largest class of differentially expressed genes (24%) in the $Nrl^{-/-}$ retina. In addition, one-third of the genes are associated with light response/vision (11%), signaling (18%) and transcription (6%). There was no significant difference between up- and down-regulated genes in terms of the specific biological processes affected; however, more genes associated with vision or cell adhesion are down-regulated in the $Nrl^{-/-}$ retina (Fig. 4). This can be attributed to greater representation of rod- rather than cone-specific transcripts on the MGU74Av2 Chips. A decreased expression of genes encoding structural proteins may reflect the abnormalities of the retinal organization in the $Nrl^{-/-}$ mouse. It should be noted that cones contain more mitochondria when compared with rods (56,57); expression changes in mitochondria associated genes (*Aqp1*, *Mscs*, *Skd3* and *Clic4*) may therefore reflect numerical and physiological differences between the populations of mitochondria in the two classes of photoreceptors.

Expanding the data set: MOE430 GeneChips and custom cDNA arrays

The MGU74Av2 GeneChip contains over 12 000 known genes and ESTs but the retina-specific transcripts are represented poorly. For example, neither Nr2e3 or cone arrestin are on these arrays. Affymetrix has since significantly improved the mouse arrays and the new MOE430 GeneChips now comprise over 36 000 genes and ESTs. These arrays are superior in design showing greater sensitivity and improved specificity of probesets. One problem with GeneChips is that the probesets are based on public databases and if transcripts are exclusively or predominantly expressed in the retina, they may not have been identified. Custom retinal cDNA arrays (28,58–60) should therefore complement GeneChip-based analysis of the $Nrl^{-/-}$ retina (J. Yu and A. Swaroop, unpublished data).

Differential expression and reactive gliosis in the $Nrl^{-/-}$ retina

The ready-extraction of rod- or cone-specific genes from the microarray analysis is complicated by the fact that the $Nrl^{-/-}$ retina undergoes a slow form of retinal degeneration (after 4–6 months, unpublished data). A marker of retinal stress, glial fibrillary acidic protein (Gfap), is up-regulated in the $Nrl^{-/-}$ retina (18). Reactive gliosis or glial hypertrophy is observed as part of the complex neuronal remodeling that occurs during retinal degeneration (61,62). Discrimination between photoreceptor-based differential expression and changes due to retinal remodeling must be evaluated carefully, especially when dealing with genes that encode proteins with a poorly defined function. One experimental strategy would be to compare gene profiles, reported here, to those of mouse models of retinal degeneration.

Cones or 'cods'

In the original characterization of the $Nrl^{-/-}$ mouse, the photoreceptor population was referred to as 'cods' as there was uncertainty as to whether the later developing but functional cones were in fact a type of hybrid photoreceptor. Subsequent analysis with cone-specific markers (such as PNA), suction electrode recordings of isolated photoreceptors (S.S. Nikonov, L. Daniele, A.J. Mears, A. Swaroop and E.N. Pugh Jr, unpublished data) and ERG of whole retina, nuclear

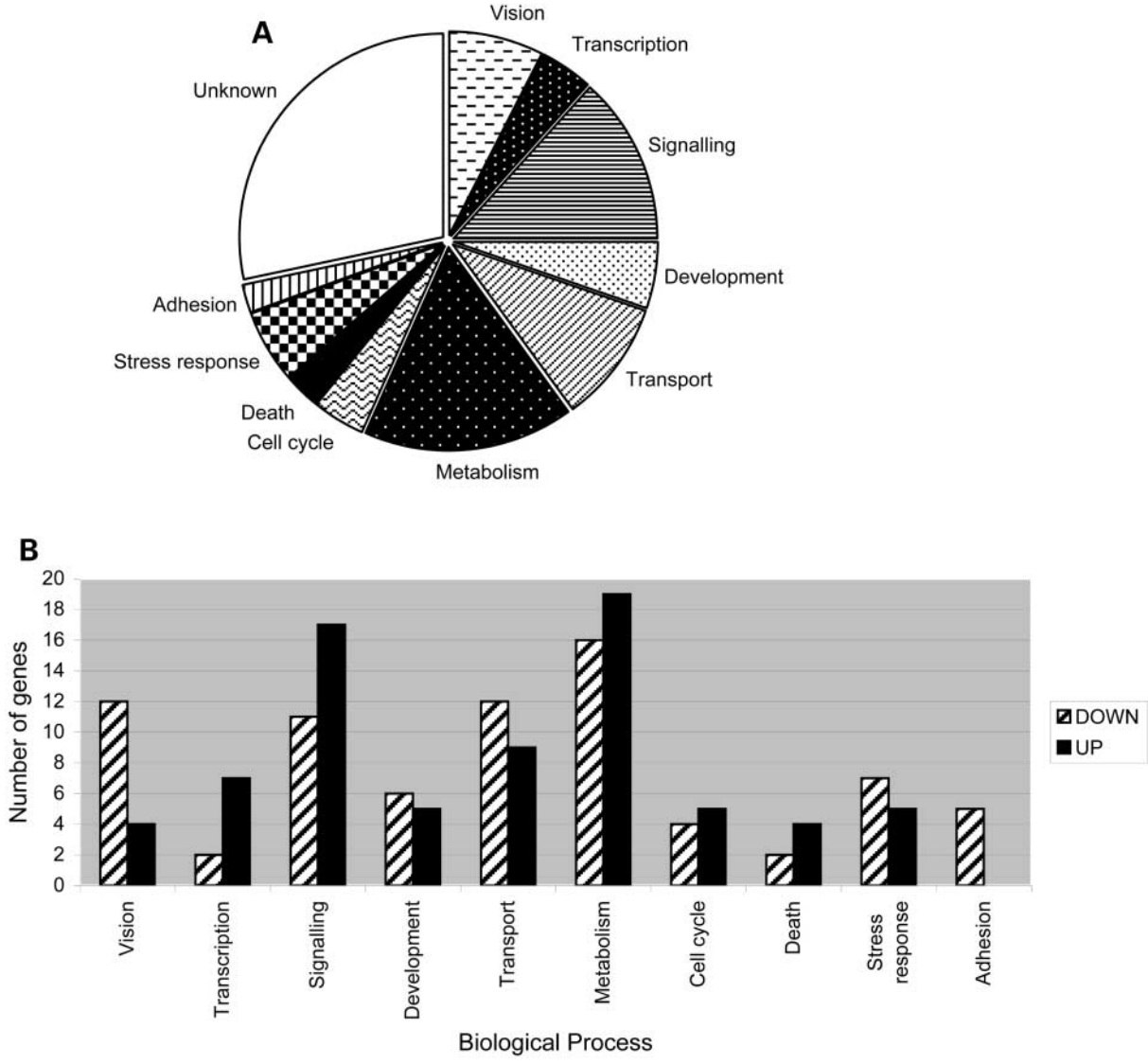

Figure 4. Biological processes associated with differentially expressed genes. (**A**) Overall distribution of all differentially expressed genes, (**B**) a comparison between up- and down-regulated genes.

morphology of the ONL (punctate staining typical of cones) and extensive molecular studies are all consistent with these photoreceptors being cones. Histologically, the retina is abnormal with rosettes and whorls disrupting the ONL, and short, sparse and disorganized OS. These changes, however, may be a consequence of inappropriate nuclear and OS packing within ONL and the sub-retinal region, and may be secondary to the actual identity and differentiation of the photoreceptors. The gene profiling data, presented here, provide strong evidence in favor of the photoreceptors of the $Nrl^{-/-}$ retina being cones and not cods.

Photoreceptor plasticity and identity

In the absence of Nrl, the failure of the retinal photoreceptors to adopt their appropriate rod identity results in their transformation into cones primarily expressing S-opsin (S-cones). Nrl therefore appears to act as a molecular switch during photoreceptor differentiation by promoting the rod differentiation program while simultaneously repressing the cone identity. The suppression of the cone fate is achieved, at least in part, through direct or indirect regulation of the transcription factor Nr2e3 (20,21), whose expression is undetectable in the $Nrl^{-/-}$ retina (18).

How does Nrl orchestrate the coordinated expression of a broad array of genes that are required for making a mature and functional rod? Delineation of direct downstream targets is the essential first step towards assembling the Nrl-mediated transcriptional regulatory network(s) underlying rod differentiation. Our study has identified several potential direct targets of Nrl by a combined approach of microarray profiling and ChIP. Several of these are known or putative transcription factors or signaling proteins that may play a role in rod or cone

differentiation. Comparative retinal gene profiling studies of mouse loss-of-function mutants of other photoreceptor transcription factors (e.g. Crx, Trβ2, Nr2e3) should provide considerable insights into the gene regulatory networks that govern differentiation and homeostasis.

MATERIALS AND METHODS

Animal use and tissue collection

University Committee on Use and Care of Animals of the University of Michigan approved all procedures involving mice. Both the $Nrl^{-/-}$ mice and the wild-type controls were of a matched mixed genetic background (R1 and C57BL/6 strains) (18). Mice were sacrificed by cervical dislocation, and the retinas were excised rapidly, frozen on dry ice and stored at −80°C. No signs of pathology were detected in any of the animals used. To isolate sufficient total RNA for labeling protocols, retinas from two mice were pooled into a single sample. To minimize false positives due to biological variation, different samples were utilized for four replicate experiments per genotype/time-point (biological replicates). For the developmental Q-PCR studies, retinas were dissected from the embryos of timed-pregnant $Nrl^{-/-}$ or wild-type females and pooled. Retinas from post-natal time-points were also pooled (entire litter) after dissection.

RNA preparation

Tissues were placed into TRIzol (Invitrogen, Carlsbad, CA, USA) (added to the frozen tissues at ∼1.3 ml per four retinas) and homogenized (Polytron, Kinematica, Lucerne, Switzerland) at maximum speed for 120 s. Subsequent steps were done according to the manufacturer's instructions.

Gene expression analysis

The GeneChips (Affymetrix, Santa Clara, CA, USA) used in the study contained ∼12 000 probe sets, corresponding to over 6000 genes and 6000 ESTs (Murine Genome U74A Array v2).

Total retinal RNA was used to generate double-stranded cDNA (ds-cDNA) with SuperScript Choice System (Invitrogen) and oligo-dT primer containing a T7 RNA polymerase promoter. After second-strand synthesis, the reaction mixture was extracted with phenol–chloroform–isoamyl alcohol, and ds-cDNA was recovered by ethanol precipitation. *In vitro* transcription was performed by using a RNA transcription labeling kit (Enzo) with 10 μl of ds-cDNA template in the presence of a mixture of unlabeled ATP, CTP, GTP and UTP and biotin-labeled CTP and UTP [bio-11-CTP and bio-16-UTP (Enzo Life Sciences, Farmingdale, NY, USA)]. Biotin-labeled cRNA was purified by using an RNeasy affinity column (Qiagen, Valencia, CA, USA), and fragmented randomly to sizes ranging from 35 to 200 bases by incubating at 94°C for 35 min. The hybridization solutions contained 100 mM MES, 1 M NaCl, 20 mM EDTA and 0.01% Tween-20. The final concentration of fragmented cRNA was 0.05 μg/μl in the hybridization solution. After hybridization, the solutions were removed and GeneChips were washed and stained with streptavidin–phycoerythrin. GeneChips were read at a resolution of 6 μm with a Hewlett-Packard GeneArray Scanner. Initial data preparation (i.e. generation of CHP files) were performed by Affymetrix MICROARRAY SUITE v5.0. Normalization (quantile method) and calculation of signal intensities were performed with the software package RMA from the R project (http://www.r-project.org/). Data were based on four Affymetrix MGU74Av2 GeneChips (biological replicates) for each time-point per genotype (i.e. total of eight GeneChips per timepoint). Of the total 24 GeneChips, only one had to be repeated due to a negative quality report based on raw image and MAS5 analysis. Ratios of average signal intensity ($\log_2$) were then calculated for the probesets ($Nrl^{-/-}$ relative to wild-type) and then converted to an AFC. Statistical validation was performed on probesets showing a minimum AFC of 1.5. If due to low signal, any of these probesets were reported as having an absent signal (based on MAS5) in all GeneChips (i.e. for both genotypes) for a given time-point then it was reported as absent and reported signal values and relative expressions were ignored.

FDR and *P*-values

The statistical method used to assign *P*-values to the fold-changes of gene responses is a two-step procedure based on the Benjamini and Yekutieli construction of FDRCI (63–65) on the fold-changes between the $Nrl^{-/-}$ and the wild-type response profiles (55). FDRCIs are $(1-q)$% confidence intervals where the level 'q' is corrected for error amplification inherent to performing multiple comparisons on many genes and many time-points. For specified minimum fold-change (fcmin) and a given level of significance q, a gene response is declared as 'positive' if the range of the FDRCI is either greater than fcmin (positive fold-change) or less than −fcmin (negative fold-change). The FDRCI *P*-value for a given gene is defined as the minimum level q for which the gene's FDRCI does not intersect the interval [−fcmin, fcmin]. For this data, we formed a ranked list of genes according to increasing FDRCI significance level having minfc of 1.5 (0.58 $\log_2$). All probesets with a *P*-value <1 were reported.

Q-PCR

RNA was treated with RQ1 DNAse (Promega, Madison, WI, USA) following manufacturer's guidelines. Oligo-dT-primed reverse transcription was performed using 2.5 μg of DNAse-treated total retinal RNA with Superscript II (Invitrogen). Primers for the validated genes were designed typically from the 3′ UTR region using Primer 3 (http://www-genome.wi.mit.edu/cgi-bin/primer/primer3). The PCR reactions on the cDNA template were then performed in triplicate in an I-cycler thermocycler with optical module (BioRad, Hercules, CA, USA). Amplified products were quantified based on the level of fluorescence of SybrGreen I (Molecular Probes, Eugene, OR, USA) in each reaction. Specificity of reactions was confirmed by melt curve analysis and gel electrophoresis. AFCs were then calculated based on the difference in the threshold cycles (C_t) between the $Nrl^{-/-}$ and the wild-type samples after normalization to *Hprt.*

Clustering analysis

Clustering based on similarity of temporal expression profiles and visualization was performed using the software program Spotfire DecisionSite 7.2 (www.spotfire.com). The signal data of statistically significant differentially expressed genes were standardized to z-scores (66), and hierarchical clustering performed using the 'Euclidean distance' method.

Annotation

Functional annotation of proteins was assigned through Gene Ontology (http://www.geneontology.org) or Locuslink (http://www.ncbi.nlm.nih.gov/LocusLink) classifications obtained through appropriate public databases such as NetAffx (http://www.netaffx.com/indexp2.jsp) (67) and DAVID (http://apps1.niaid.nih.gov/david/upload.asp) (68).

ChIP analysis

Retinas were obtained from the C57BL/6 wild-type mice and snap frozen on dry ice. ChIP was performed using a commercial assay kit (Upstate Biotechnologies, Charlottesville, VA, USA). Briefly, four retinas were crosslinked in PBS containing proteinase inhibitors and a final concentration of 1% formaldehyde for 15 min at 37°C. The retinas were washed four times in ice-cold PBS with proteinase inhibitors and then incubated on ice for 15 min. The tissue was then sonicated on ice with 10 pulses of 20 sec. The remaining steps were performed as described by the manufacturer, using an anti-NRL polyclonal antibody (8).

The putative promoter region for each of the genes analyzed was determined using *in silico* methods (http://www.ncbi.nlm.nih.gov/mapview). Each promoter DNA sequence was analyzed using Matinspector (http://www.genomatix.de/index.html) and PCR primers were designed to flank putative AP1-like sites either predicted by Matinspector or predicted manually. If there was more than one AP-1 like site, the sequence element closest to the 5′ untranslated sequence was used. Equal amounts of input DNA, with and without antibody, were used in each PCR reaction.

SUPPLEMENTARY MATERIAL

Supplementary Material is available at HMG Online.

ACKNOWLEDGEMENTS

The authors thank S. Zareparsi, M.I. Othman and S.P. MacNee for discussions, and Sharyn Ferrara for administrative assistance. This research was supported by grants from the National Institutes of Health (EY11115 including administrative supplements, EY07003), The Foundation Fighting Blindness (Owings Mills, MD, USA) and Research to Prevent Blindness (RPB; New York, NY, USA). A.J.M is a recipient of a Tier 2 Canada Research Chair. J.S.F. is a recipient of an FFB-Canada post-doctoral fellowship. A.S. is Harold F. Falls Collegiate Professor and RPB Senior Scientific Investigator.

REFERENCES

1. Masland, R.H. (2001) The fundamental plan of the retina. *Nat. Neurosci.*, **4**, 877–886.
2. Curcio, C.A., Sloan, K.R., Kalina, R.E. and Hendrickson, A.E. (1990) Human photoreceptor topography. *J. Comp. Neurol.*, **292**, 497–523.
3. Williams, D.S. (2002) Transport to the photoreceptor outer segment by myosin VIIa and kinesin II. *Vision Res.*, **42**, 455–462.
4. Tan, E., Wang, Q., Quiambao, A.B., Xu, X., Qtaishat, N.M., Peachey, N.S., Lem, J., Fliesler, S.J., Pepperberg, D.R., Naash, M.I. *et al.* (2001) The relationship between opsin overexpression and photoreceptor degeneration. *Invest. Ophthalmol. Vis. Sci.*, **42**, 589–600.
5. Pacione, L.R., Szego, M.J., Ikeda, S., Nishina, P.M. and McInnes, R.R. (2003) Progress toward understanding the genetic and biochemical mechanisms of inherited photoreceptor degenerations. *Annu. Rev. Neurosci.*, **26**, 657–700.
6. Rattner, A., Sun, H. and Nathans, J. (1999) Molecular genetics of human retinal disease. *Annu. Rev. Genet.*, **33**, 89–131.
7. Swaroop, A., Xu, J.Z., Pawar, H., Jackson, A., Skolnick, C. and Agarwal, N. (1992) A conserved retina-specific gene encodes a basic motif/leucine zipper domain. *Proc. Natl Acad. Sci. USA*, **89**, 266–270.
8. Swain, P.K., Hicks, D., Mears, A.J., Apel, I.J., Smith, J.E., John, S.K., Hendrickson, A., Milam, A.H. and Swaroop, A. (2001) Multiple phosphorylated isoforms of NRL are expressed in rod photoreceptors. *J. Biol. Chem.*, **276**, 36824–36830.
9. Mitton, K.P., Swain, P.K., Chen, S., Xu, S., Zack, D.J. and Swaroop, A. (2000) The leucine zipper of NRL interacts with the CRX homeodomain. A possible mechanism of transcriptional synergy in rhodopsin regulation. *J. Biol. Chem.*, **275**, 29794–29799.
10. Rehemtulla, A., Warwar, R., Kumar, R., Ji, X., Zack, D.J. and Swaroop, A. (1996) The basic motif-leucine zipper transcription factor Nrl can positively regulate rhodopsin gene expression. *Proc. Natl Acad. Sci. USA*, **93**, 191–195.
11. Pittler, S.J., Zhang, Y., Chen, S., Mears, A.J., Zack, D.J., Ren, Z., Swain, P.K., Yao, S., Swaroop, A. and White, J.B. (2004) Functional analysis of the rod photoreceptor cGMP phosphodiesterase alpha subunit gene promoter: Nrl and Crx are required for full transcriptional activity. *J. Biol. Chem.*, **279**, 19800–19807.
12. Lerner, L.E., Gribanova, Y.E., Ji, M., Knox, B.E. and Farber, D.B. (2001) Nrl and Sp nuclear proteins mediate transcription of rod-specific cGMP-phosphodiesterase beta-subunit gene: involvement of multiple response elements. *J. Biol. Chem.*, **276**, 34999–35007.
13. Bessant, D.A., Payne, A.M., Mitton, K.P., Wang, Q.L., Swain, P.K., Plant, C., Bird, A.C., Zack, D.J., Swaroop, A. and Bhattacharya, S.S. (1999) A mutation in NRL is associated with autosomal dominant retinitis pigmentosa. *Nat. Genet.*, **21**, 355–356.
14. Bessant, D.A., Payne, A.M., Plant, C., Bird, A.C., Swaroop, A. and Bhattacharya, S.S. (2000) NRL S50T mutation and the importance of 'founder effects' in inherited retinal dystrophies. *Eur. J. Hum. Genet.*, **8**, 783–787.
15. DeAngelis, M.M., Grimsby, J.L., Sandberg, M.A., Berson, E.L. and Dryja, T.P. (2002) Novel mutations in the NRL gene and associated clinical findings in patients with dominant retinitis pigmentosa. *Arch. Ophthalmol.*, **120**, 369–375.
16. Martinez-Gimeno, M., Maseras, M., Baiget, M., Beneito, M., Antinolo, G., Ayuso, C. and Carballo, M. (2001) Mutations P51U and G122E in retinal transcription factor NRL associated with autosomal dominant and sporadic retinitis pigmentosa. *Hum. Mutat.*, **17**, 520.
17. Bessant, D.A., Holder, G.E., Fitzke, F.W., Payne, A.M., Bhattacharya, S.S. and Bird, A.C. (2003) Phenotype of retinitis pigmentosa associated with the Ser50Thr mutation in the NRL gene. *Arch. Ophthalmol.*, **121**, 793–802.
18. Mears, A.J., Kondo, M., Swain, P.K., Takada, Y., Bush, R.A., Saunders, T.L., Sieving, P.A. and Swaroop, A. (2001) Nrl is required for rod photoreceptor development. *Nat. Genet.*, **29**, 447–452.
19. Akhmedov, N.B., Piriev, N.I., Chang, B., Rapoport, A.L., Hawes, N.L., Nishina, P.M., Nusinowitz, S., Heckenlively, J.R., Roderick, T.H., Kozak, C.A. *et al.* (2000) A deletion in a photoreceptor-specific nuclear receptor mRNA causes retinal degeneration in the rd7 mouse. *Proc. Natl Acad. Sci. USA*, **97**, 5551–5556.
20. Haider, N.B., Naggert, J.K. and Nishina, P.M. (2001) Excess cone cell proliferation due to lack of a functional NR2E3 causes retinal dysplasia and degeneration in rd7/rd7 mice. *Hum. Mol. Genet.*, **10**, 1619–1626.

21. Haider, N.B., Jacobson, S.G., Cideciyan, A.V., Swiderski, R., Streb, L.M., Searby, C., Beck, G., Hockey, R., Hanna, D.B., Gorman, S. *et al.* (2000) Mutation of a nuclear receptor gene, *NR2E3*, causes enhanced S cone syndrome, a disorder of retinal cell fate. *Nat. Genet.*, **24**, 127–131.
22. Livesey, F.J. and Cepko, C.L. (2001) Vertebrate neural cell-fate determination: lessons from the retina. *Nat. Rev. Neurosci.*, **2**, 109–118.
23. Nishida, A., Furukawa, A., Koike, C., Tano, Y., Aizawa, S., Matsuo, I. and Furukawa, T. (2003) Otx2 homeobox gene controls retinal photoreceptor cell fate and pineal gland development. *Nat. Neurosci.*, **6**, 1255–1263.
24. Ng, L., Hurley, J.B., Dierks, B., Srinivas, M., Salto, C., Vennstrom, B., Reh, T.A. and Forrest, D. (2001) A thyroid hormone receptor that is required for the development of green cone photoreceptors. *Nat. Genet.*, **27**, 94–98.
25. Zhang, J., Gray, J., Wu, L., Leone, G., Rowan, S., Cepko, C.L., Zhu, X., Craft, C.M. and Dyer, M.A. (2004) Rb regulates proliferation and rod photoreceptor development in the mouse retina. *Nat. Genet.*, **36**, 351–360.
26. DeRyckere, D. and DeGregori, J. (2002) Identification and characterization of transcription factor target genes using gene-targeted mice. *Methods*, **26**, 57–75.
27. Livesey, F.J., Furukawa, T., Steffen, M.A., Church, G.M. and Cepko, C.L. (2000) Microarray analysis of the transcriptional network controlled by the photoreceptor homeobox gene *Crx*. *Curr. Biol.*, **10**, 301–310.
28. Mu, X., Zhao, S., Pershad, R., Hsieh, T.F., Scarpa, A., Wang, S.W., White, R.A., Beremand, P.D., Thomas, T.L., Gan, L. *et al.* (2001) Gene expression in the developing mouse retina by EST sequencing and microarray analysis. *Nucl. Acids Res.*, **29**, 4983–4993.
29. Irizarry, R.A., Bolstad, B.M., Collin, F., Cope, L.M., Hobbs, B. and Speed, T.P. (2003) Summaries of Affymetrix GeneChip probe level data. *Nucl. Acids Res.*, **31**, e15.
30. Young, R.W. (1985) Cell differentiation in the retina of the mouse. *Anat. Rec.*, **212**, 199–205.
31. Irizarry, R.A., Hobbs, B., Collin, F., Beazer-Barclay, Y.D., Antonellis, K.J., Scherf, U. and Speed, T.P. (2003) Exploration, normalization, and summaries of high density oligonucleotide array probe level data. *Biostatistics*, **4**, 249–264.
32. Barash, Y., Dehan, E., Krupsky, M., Franklin, W., Geraci, M., Friedman, N. and Kaminski, N. (2004) Comparative analysis of algorithms for signal quantitation from oligonucleotide microarrays. *Bioinformatics*, **20**, 839–846.
33. Xi, J., Farjo, R., Yoshida, S., Kern, T.S., Swaroop, A. and Andley, U.P. (2003) A comprehensive analysis of the expression of crystallins in mouse retina. *Mol. Vis.*, **9**, 410–419.
34. Kennan, A., Aherne, A., Palfi, A., Humphries, M., McKee, A., Stitt, A., Simpson, D.A., Demtroder, K., Orntoft, T., Ayuso, C. *et al.* (2002) Identification of an IMPDH1 mutation in autosomal dominant retinitis pigmentosa (RP10) revealed following comparative microarray analysis of transcripts derived from retinas of wild-type and Rho(−/−) mice. *Hum. Mol. Genet.*, **11**, 547–557.
35. Taylor, R.E., Shows, K.H., Zhao, Y. and Pittler, S.J. (2001) A PDE6A promoter fragment directs transcription predominantly in the photoreceptor. *Biochem. Biophys. Res. Commun.*, **282**, 543–547.
36. Payne, A.M., Downes, S.M., Bessant, D.A., Taylor, R., Holder, G.E., Warren, M.J., Bird, A.C. and Bhattacharya, S.S. (1998) A mutation in guanylate cyclase activator 1A (GUCA1A) in an autosomal dominant cone dystrophy pedigree mapping to a new locus on chromosome 6p21.1. *Hum. Mol. Genet.*, **7**, 273–277.
37. Downes, S.M., Holder, G.E., Fitzke, F.W., Payne, A.M., Warren, M.J., Bhattacharya, S.S. and Bird, A.C. (2001) Autosomal dominant cone and cone–rod dystrophy with mutations in the guanylate cyclase activator 1A gene-encoding guanylate cyclase activating protein-1. *Arch. Ophthalmol.*, **119**, 96–105.
38. Naya, F.S. and Olson, E. (1999) MEF2: a transcriptional target for signaling pathways controlling skeletal muscle growth and differentiation. *Curr. Opin. Cell Biol.*, **11**, 683–688.
39. Parker, M.H., Seale, P. and Rudnicki, M.A. (2003) Looking back to the embryo: defining transcriptional networks in adult myogenesis. *Nat. Rev. Genet.*, **4**, 497–507.
40. Mori, M., Ghyselinck, N.B., Chambon, P. and Mark, M. (2001) Systematic immunolocalization of retinoid receptors in developing and adult mouse eyes. *Invest. Ophthalmol. Vis. Sci.*, **42**, 1312–1318.
41. Li, A., Zhu, X., Brown, B. and Craft, C.M. (2003) Gene expression networks underlying retinoic acid-induced differentiation of human retinoblastoma cells. *Invest. Ophthalmol. Vis. Sci.*, **44**, 996–1007.
42. Mollereau, B., Dominguez, M., Webel, R., Colley, N.J., Keung, B., de Celis, J.F. and Desplan, C. (2001) Two-step process for photoreceptor formation in *Drosophila*. *Nature*, **412**, 911–913.
43. Leong, M.L., Maiyar, A.C., Kim, B., O'Keeffe, B.A. and Firestone, G.L. (2003) Expression of the serum- and glucocorticoid-inducible protein kinase, Sgk, is a cell survival response to multiple types of environmental stress stimuli in mammary epithelial cells. *J. Biol. Chem.*, **278**, 5871–5882.
44. Heyninck, K., De Valck, D., Vanden Berghe, W., Van Criekinge, W., Contreras, R., Fiers, W., Haegeman, G. and Beyaert, R. (1999) The zinc finger protein A20 inhibits TNF-induced NF-kappaB-dependent gene expression by interfering with an RIP- or TRAF2-mediated transactivation signal and directly binds to a novel NF-kappaB-inhibiting protein ABIN. *J. Cell Biol.*, **145**, 1471–1482.
45. Wu, T., Chiang, S.K., Chau, F.Y. and Tso, M.O. (2003) Light-induced photoreceptor degeneration may involve the NF kappa B/caspase-1 pathway *in vivo*. *Brain Res.*, **967**, 19–26.
46. Jastrzebska, B., Filipek, A., Nowicka, D., Kaczmarek, L. and Kuznicki, J. (2000) Calcyclin (S100A6) binding protein (CacyBP) is highly expressed in brain neurons. *J. Histochem. Cytochem.*, **48**, 1195–1202.
47. Joo, J.H., Kim, J.W., Lee, Y., Yoon, S.Y., Kim, J.H., Paik, S.G. and Choe, I.S. (2003) Involvement of NF-kappaB in the regulation of S100A6 gene expression in human hepatoblastoma cell line HepG2. *Biochem. Biophys. Res. Commun.*, **307**, 274–280.
48. Claudepierre, T., Dalloz, C., Mornet, D., Matsumura, K., Sahel, J. and Rendon, A. (2000) Characterization of the intermolecular associations of the dystrophin-associated glycoprotein complex in retinal Muller glial cells. *J. Cell Sci.*, **113**, 3409–3417.
49. Claudepierre, T., Rodius, F., Frasson, M., Fontaine, V., Picaud, S., Dreyfus, H., Mornet, D. and Rendon, A. (1999) Differential distribution of dystrophins in rat retina. *Invest. Ophthalmol. Vis. Sci.*, **40**, 1520–1529.
50. Ribelayga, C., Wang, Y. and Mangel, S.C. (2004) A circadian clock in the fish retina regulates dopamine release via activation of melatonin receptors. *J. Physiol.*, **554**, 467–482.
51. Tosini, G. and Fukuhara, C. (2003) Photic and circadian regulation of retinal melatonin in mammals. *J. Neuroendocrinol.*, **15**, 364–369.
52. Dorrell, M.I., Aguilar, E., Weber, C. and Friedlander, M. (2004) Global gene expression analysis of the developing post natal mouse retina. *Invest. Ophthalmol. Vis. Sci.*, **45**, 1009–1019.
53. Kremerskothen, J., Plaas, C., Buther, K., Finger, I., Veltel, S., Matanis, T., Liedtke, T. and Barnekow, A. (2003) Characterization of KIBRA, a novel WW domain-containing protein. *Biochem. Biophys. Res. Commun.*, **300**, 862–867.
54. Zareparsi, S., Hero, A.O., Zack, D.J., Williams, R.W. and Swaroop, A. (2004) Seeing the unseen: Microarray-based gene expression profiling in vision. *Invest. Ophthalmol. Vis. Sci.*, in press.
55. Hero, A.O., Fleury, G., Mears, A.J. and Swaroop, A. (2004) Multicriteria gene screening for analysis of differential expression with DNA microarrays. *EURASIP JASP*, **2004**, 43–52.
56. Hoang, Q.V., Linsenmeier, R.A., Chung, C.K. and Curcio, C.A. (2002) Photoreceptor inner segments in monkey and human retina: mitochondrial density, optics, and regional variation. *Vis. Neurosci.*, **19**, 395–407.
57. Perkins, G.A., Ellisman, M.H. and Fox, D.A. (2003) Three-dimensional analysis of mouse rod and cone mitochondrial cristae architecture: bioenergetic and functional implications. *Mol. Vis.*, **9**, 60–73.
58. Farjo, R., Yu, J., Othman, M.I., Yoshida, S., Sheth, S., Glaser, T., Baehr, W. and Swaroop, A. (2002) Mouse eye gene microarrays for investigating ocular development and disease. *Vision Res.*, **42**, 463–470.
59. Chowers, I., Gunatilaka, T.L., Farkas, R.H., Qian, J., Hackam, A.S., Duh, E., Kageyama, M., Wang, C., Vora, A., Campochiaro, P.A. *et al.* (2003) Identification of novel genes preferentially expressed in the retina using a custom human retina cDNA microarray. *Invest. Ophthalmol. Vis. Sci.*, **44**, 3732–3741.
60. Mu, X., Beremand, P.D., Zhao, S., Pershad, R., Sun, H., Scarpa, A., Liang, S., Thomas, T.L. and Klein, W.H. (2004) Discrete gene sets depend on POU domain transcription factor Brn3b/Brn-3.2/POU4f2 for their

expression in the mouse embryonic retina. *Development*, **131**, 1197–1210.
61. Jones, B.W., Watt, C.B., Frederick, J.M., Baehr, W., Chen, C.K., Levine, E.M., Milam, A.H., Lavail, M.M. and Marc, R.E. (2003) Retinal remodeling triggered by photoreceptor degenerations. *J. Comp. Neurol.*, **464**, 1–16.
62. Marc, R.E., Jones, B.W., Watt, C.B. and Strettoi, E. (2003) Neural remodeling in retinal degeneration. *Prog. Retin. Eye Res.*, **22**, 607–655.
63. Reiner, A., Yekutieli, D. and Benjamini, Y. (2003) Identifying differentially expressed genes using false discovery rate controlling procedures. *Bioinformatics*, **19**, 368–375.
64. Benjamini, Y., Drai, D., Elmer, G., Kafkafi, N. and Golani, I. (2001) Controlling the false discovery rate in behavior genetics research. *Behav. Brain Res.*, **125**, 279–284.
65. Benjamini, Y. and Hochberg, Y. (1995) Controlling the false discovery rate: a practical and powerful approach to multiple testing. *J. R. Stat. Soc.*, **57**, 289–300.
66. Matoba, R., Kato, K., Kurooka, C., Maruyama, C., Sakakibara, Y. and Matsubara, K. (2000) Correlation between gene functions and developmental expression patterns in the mouse cerebellum. *Eur. J. Neurosci.*, **12**, 1357–1371.
67. Liu, G., Loraine, A.E., Shigeta, R., Cline, M., Cheng, J., Valmeekam, V., Sun, S., Kulp, D. and Siani-Rose, M.A. (2003) NetAffx: Affymetrix probesets and annotations. *Nucl. Acids Res.*, **31**, 82–86.
68. Dennis, G., Jr, Sherman, B.T., Hosack, D.A., Yang, J., Gao, W., Lane, H.C. and Lempicki, R.A. (2003) DAVID: database for annotation, visualization, and integrated discovery. *Genome Biol.*, **4**, P3.